ADVANCED MATERIALS
www.advmat.de

# Nanoparticle-Based Bioaffinity Assays: From the Research Laboratory to the Market

*Zdeněk Farka, Julian C. Brandmeier, Matthias J. Mickert, Matěj Pastucha, Karel Lacina, Petr Skládal, Tero Soukka, and Hans H. Gorris**

**Advances in the development of new biorecognition elements, nanoparticle-based labels as well as instrumentation have inspired the design of new bioaffinity assays. This review critically discusses the potential of nanoparticles to replace current enzymatic or molecular labels in immunoassays and other bioaffinity assays. Successful implementations of nanoparticles in commercial assays and the need for rapid tests incorporating nanoparticles in different roles such as capture support, signal generation elements, and signal amplification systems are highlighted. The limited number of nanoparticles applied in current commercial assays can be explained by challenges associated with the analysis of real samples (e.g., blood, urine, or nasal swabs) that are difficult to resolve, particularly if the same performance can be achieved more easily by conventional labels. Lateral flow assays that are based on the visual detection of the red-colored line formed by colloidal gold are a notable exception, exemplified by SARS-CoV-2 rapid antigen tests that have moved from initial laboratory testing to widespread market adaption in less than two years.**

## 1. Introduction

Progress in the design, controlled synthesis, and mass production of nanoparticles (NPs) has gained momentum since the turn of the century, and NPs have found their way into numerous commercial products and have permeated our everyday life—for good or bad. In the analytical sciences, however, NPs offer tremendous potential for addressing real-world problems in medical diagnosis, food safety, and environmental monitoring. Consequently, NPs displaying novel optical, electrochemical, or catalytic features have been continuously employed to improve the performance of established bioaffinity assays and to develop entirely new detection schemes. Other applications of NPs for therapeutic technologies[1] and imaging[2] are beyond the scope of this review.

Although there are thousands of research articles on the application of NPs for sensing and imaging every year, only some of these go beyond proof-of-principle studies and are patented, and even fewer find their way into the market. Many reviews have been published to keep up with the large number of original research articles on new NP-based detection schemes.[3–5] There is, however, a need for a critical evaluation of the most suitable approaches for commercialization because many recent materials-oriented papers have claimed analysis capabilities that are either impractical, are not tested for selectivity, or are otherwise deficient.

Scientific publications typically focus on the performance of the detection element to show the highest sensitivity of newly developed assay systems under ideal experimental conditions, e.g., by using commercially available bioaffinity reagents and standard

Z. Farka, J. C. Brandmeier, M. Pastucha, P. Skládal, H. H. Gorris
Department of Biochemistry
Faculty of Science
Masaryk University
Kamenice 5, Brno 625 00, Czech Republic
E-mail: gorris@mail.muni.cz

J. C. Brandmeier
Institute of Analytical Chemistry, Chemo- and Biosensors
University of Regensburg
Universitätsstr. 31, 93053 Regensburg, Germany

M. J. Mickert
Lumito AB
Mårtenstorget 5, Lund 223 51, Sweden

M. Pastucha
TestLine Clinical Diagnostics
Křižíkova 188, Brno 612 00, Czech Republic

K. Lacina
CEITEC–Central European Institute of Technology
Masaryk University
Kamenice 5, Brno 625 00, Czech Republic

T. Soukka
Department of Life Technologies/Biotechnology
University of Turku
Kiinamyllynkatu 10, Turku 20520, Finland

The ORCID identification number(s) for the author(s) of this article can be found under https://doi.org/10.1002/adma.202307653



**DOI: 10.1002/adma.202307653**

buffers instead of real samples. Thus, they cover only two of the key elements important for commercialization. A robust, i.e., an assay without matrix effects, fast, and simple, i.e., user friendly, performance ideally at the test site (point-of-care, PoC) without the need of trained specialists, however, is in most cases more important than the lowest possible limit of detection (LOD). A paradigmatic example for PoC tests is the lateral flow assay (LFA) using gold nanoparticles (AuNPs) for a direct visual detection by the naked eye.[6] LFAs for pregnancy testing have already been on the market since the 1970s,[7] but routine testing using rapid Covid-19 antigen LFAs has become even more important for our daily life. Such rapid tests are a good illustration that PoC testing had an even greater effect on controlling the Covid-19 pandemic than more sensitive PCR tests that need to be performed in a centralized laboratory. Even though the Covid-19 pandemic ended, the world market revenues for LFAs are expected to increase from $20.5 billion in 2022 to $22.6 billion in 2027.[8]

This review aims to serve as a guideline 1) to distinguish between NP-based bioaffinity assays that are nonproductive, i.e., where existing methods are satisfactory or better, and that are productive, i.e., where the properties of NPs address challenges and limitation of current methods, 2) to understand what is required for developing assays and sensors that optimally address the needs and limitations of potential end users, e.g., in PoC tests or diagnostic laboratories, and 3) to encourage researchers to go beyond proof-of-concept studies by testing more relevant samples. A discussion on the challenges associated with microfluidic PoC devices that have led to limited commercial success was published earlier.[9]

For the commercialization of NP-based bioaffinity assays, we have to consider four key elements: 1) performance and complexity of the detection element that determine the readout mechanism and thus the instrument requirements, 2) user-friendliness including assay time and throughput, 3) specificity of the bioaffinity reagent/receptor, and 4) absence of interferences, which has been defined as "the effect of a substance present in an analytical system which causes a deviation of the measured value from the true value, usually expressed as concentration or activity."[10] In diagnostic applications, the target analytes are typically contained in complex matrices such as blood, where preanalytical variability may arise from blood collection, the nature of the sample, hemolysis, lipaemia, stability, and storage. Additionally, blood is a notorious source of matrix effects[11] caused by serum proteins such as albumin, fibrinogen, rheumatoid factors, complement, lysozyme, endogenous hormone-binding proteins, autoantibodies, and heterophilic antibodies. Reagents such as buffers, monoclonal/polyclonal antibodies or detection labels may show different levels of nonspecific interactions with the components of the complex sample as well as other assay reagents, which are important factors to consider during optimization steps. Furthermore, immunoassays may show a hook effect when analyte concentrations are too high.[10] Nonspecific binding of species that are not targeted by the affinity reagent as well as label components limit the sensitivity and specificity of all assays. NP-based labels, however, can be particularly challenging in this regard because of their larger interacting surface area as compared to molecular labels.[12]

This review primarily discusses NPs that are smaller than 100 nm in diameter as labels and/or transducers in contrast to, e.g., magnetic microspheres (beads) that are typically much larger and serve as capture surfaces. Several types of NPs afford distinct optical features that are advantageous for assays and sensing and cannot be achieved by using molecular labels (yet). For example, 1) semiconductor NPs show a size-dependent quantum confinement (quantum dots) and tunable emission wavelength, 2) photon-upconversion nanoparticles (UCNPs) are excited by long-wavelength light and emit shorter wavelength light (anti-Stokes emission), which avoids background fluorescence and light scattering, and 3) noble metal NPs exhibit localized surface plasmon resonance, which depends on the metal species, aggregation and size of the NPs.

In addition to these specific advantages, the larger size of NPs compared to molecular labels confers some general advantages. 1) Compared to individually labeled binder molecules, NPs can be conjugated to low-affinity binders, such as lectins or peptides, which result in an affinity enhancement due to its effect on both kinetics (lower dissociation rate) and avidity (polyvalent binding).[13,14] 2) The attainable signal from a single NP is typically much stronger than the signal from a single molecular label such that the detection of individual immune complexes becomes possible by using relatively simple means.[15] 3) NPs are typically (photo)chemically more stable and their properties are typically less affected by the chemical environment compared to molecular labels. The robustness under ambient conditions is a particular advantage of NPs compared to the more common biochemical detection reagents such as enzymes.

On the other hand, the application of NPs is associated with some challenges. 1) The synthesis of NPs is more difficult and even if it leads to a homogeneous batch there is still some variability in the number of atoms contained in a population of NPs unlike molecular labels that are chemically identical if properly purified. 2) The larger size of NPs may lead to steric hindrance during affinity binding, and 3) the limited colloidal stability and shelf-life affect their commercialization. To address these challenges, a well-designed surface architecture of NPs is essential.[16] Additionally, 4) the potential (nano)toxicity has been increasingly in the focus of attention.[17]

## 2. Fields of Application and User Demands

The field of application and intended purpose of the analysis determine how fast an analyte must be detectable. For example, the cardiac biomarker human cardiac troponin must be detectable on-site as every minute counts in beginning the life-saving treatment. Annually, more than one million deaths in the US are caused by coronary artery diseases, especially acute myocardial infarction.[18] With hospitals often overcrowded and staff shortages, there is a significant market need for a rapid analyzer that can help diagnose patients on site. The detection of biological or chemical warfare agents also requires immediate safety arrangements at the site of exposure. Similarly, imported meat and other food products require rapid control before delivery to the customers. All these are examples where decentralized analysis and PoC devices are urgently required because central laboratory testing depends on the sample transfer and is too slow to respond.

The containment of the recent Covid-19 pandemic also relied on a rapid and tight surveillance by PoC tests. Home testing with PoC devices avoided unnecessary travels to health care

units for sample delivery and assisted in limiting the exposures and transmission of the infection. Other diseases such as sexually transmitted diseases have longer cycles of infection and/or are not transmitted as easily as viruses released from the respiratory tract. Nevertheless, also there a tight control is preferred, highlighting the general need for rapid PoC tests. NP-based LFAs are cheap, fast, user-friendly and in the simplest case the result can be read out by eye or by using a mobile phone and thus are a cornerstone for PoC testing outside of the laboratory.[19,20]

By contrast, the detection of cancer markers typically does not require short turnaround times and can be performed within one week in a hospital laboratory. While screening of cancer biomarkers for cancer prevention is very important, PoC cancer tests are not 100% specific because many other factors, e.g., benign tumors, can lead to elevated biomarker concentrations. Consequently, the results of these home tests would still need to be confirmed with the doctor or the test result is directly sent to the doctor via the smartphone, and the likelihood of false positive results lead to unnecessary psychological stress. Van Poppel et al.[21] also showed that the inefficient use of already existing screening tools is more problematic than the lack of new ones. Nevertheless, in some cases screening of cancer markers may be useful. For example, after radical prostatectomy the cancer marker prostate-specific antigen (PSA) should no longer be detectable. Therefore, regular checkups are required to monitor increasing PSA levels as an indicator of recurring prostate cancer.

OPKO Health offers the Claros 1 analyzer and a credit card-sized microfluidic cassette for the fast determination of total PSA from a finger prick blood sample amenable to PoC applications. PSA in the blood sample binds to an AuNP-labeled detection antibody in the cassette, which is inserted into the Claros 1 analyzer. The sample is pulled over a test zone by applying a vacuum to the microfluidic channel. The AuNP-labeled detection antibody, PSA, and an immobilized second anti-PSA antibody form a sandwich complex on the test zone. To enhance the optical density around the immune complexes, a silver amplification step is performed where $Ag^+$ is reduced to Ag, which precipitates on the AuNPs and attenuates the light transmission through the test zone.[22]

The type of analyte also determines which assay parameters are most important: the assays for diseases requiring immediate action should have short turnaround time to enable an immediate beginning of treatment. In the case of cancer markers, where early detection is also important, it is however not the speed of assay, but rather the LOD that is more relevant. In case of the pregnancy test, the detection of relatively high concentrations of human chorionic gonadotropin is sufficient. It is important for the user that the stronger color change afforded by NPs renders the visual interpretation easier. Otherwise, these tests are optimal for home testing because they are easy to use and do not need any instrumental support. Consequently, there is no need to further improve the speed or sensitivity of the over-the-counter pregnancy test.

Optimizing the LOD also bears another implication: if the LOD of an assay is improved even though current assays are sufficient for the analyte detection, it may still be possible to improve the overall assay performance because diluting the sample further before running the assay also reduces possible matrix effects. On the other hand, for assays with short turn-around-time as needed for troponin, it is advantageous to minimize any sample processing and dilution steps to keep the time for obtaining the test result as short as possible. In this case, performing the assay in undiluted and unprocessed whole blood is advantageous.

## 3. Key Performance Parameters of Nanoparticle-Based Bioassays

NPs and their bioconjugates employed in commercial immunoassay platforms are typically smaller than 100 nm in diameter, but there are also examples of platforms with significantly larger particles such as ceramic upconversion particles of 400 nm in diameter.[23] The signal quantity obtainable from the NPs by an optical measurement commonly depends on their volumetric dimension, i.e., larger NPs typically generate a stronger signal, which is more easily detectable, but there are several exceptions such as quantum dots (QDs)[24] and light scattering or plasmonic metal NPs.[25] **Figure 1** shows the diversity of NP-based bioaffinity assay amenable to the detection of structurally diverse analytes.

In addition to the average diameter, also the shape of NP-based labels is important for the reactivity of the bioconjugates. NP labels of spherical shape and coated uniformly with specific binders on their surface are considered optimal because they are independent of the NP orientation. Such labels bind their targets more homogeneously with minimal NP reorientation, which avoids different steric restrictions on binder molecules attached to different locations on the NP surface. Thus, the ideal NP label should be spherical in shape and its size should be as close as possible to molecular labels while providing the advantages and composition of larger nanostructure—which practically cannot be achieved at the same time. It is relatively easy to achieve a highly spherical shape for larger NPs synthesized from organic polymers or silica, but in case of small AuNPs[26] or inorganic crystalline NPs such as UCNPs[27] a completely spherical shape is more challenging.

NPs employed in clinical assays also inevitably interact with bulk proteins present in the serum sample. Proteins more or less weakly adsorbed to the NP surface form a so-called protein corona, which sterically hinders specific interactions of the surface-bound antibodies with the analytes and affects the assay response.[28] Advances in the surface functionalization using highly hydrophilic polymer coatings such as dextran[29] minimize the formation of a protein corona, improve resistance against fouling and minimize the nonspecific interactions of the NP labels when analyzing complex samples.[30] Other biochemical approaches have aimed to obtain a high surface coverage of affinity binders with an optimized orientation.[31] The optimal arrangement of affinity binders has the potential to improve the overall assay performance and reduces the possibility of false-positive results.

Finally, the much larger size of NP labels compared to molecular labels renders NP labels intrinsically more prone to aggregation and sedimentation. Thus, the long-term colloidal stability of NP labels has to be confirmed over long times and for several batches before market introduction. This aspect has been often neglected in fundamental research studies, where new batches of NPs can be prepared more easily on a smaller scale. Dry chemistry-based approaches eliminate problems with solution-based particle-containing reagents.[32,33] For example, the

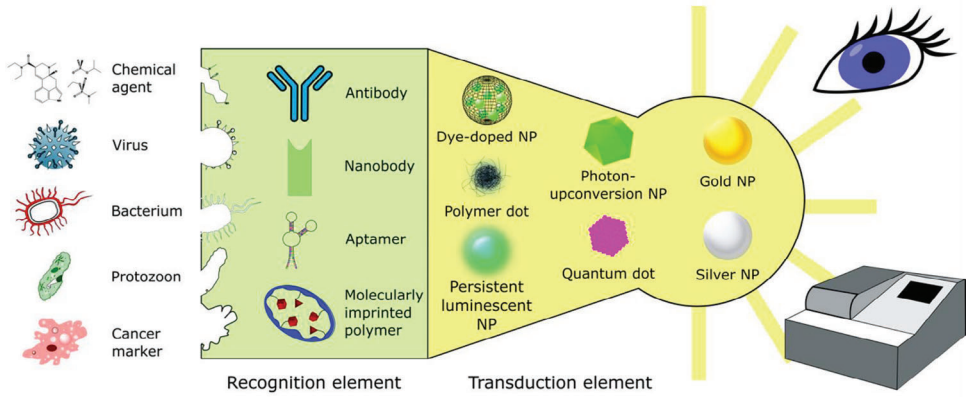


**Figure 1.** Scheme of bioaffinity assay containing different possible affinity binders as the recognition element and various optical NP labels as the transduction element. Ideally, the presence of the analyte is directly detected by the naked eye. By contrast, readout instruments are typically much more sensitive depending on the chosen transduction element.

industrial production of most LFAs already includes drying of the NP labels on the conjugate pad, which enables more flexible storage under ambient conditions. The use of dried NP labels is also applicable to other assay platforms.

The following sections describe selected examples of commercial NP-based labels and assays that are summarized in **Table 1**. The worldwide number of companies, however, is by far too large to include them all.

### 3.1. Analyte Sampling

A representative analyte sampling and extraction is of paramount importance for the overall assay performance. Analyte sampling strongly depends on the application area. For example, in clinical assays, the classic sample is blood serum in which mainly target proteins are detected, but also small molecules, such as hormones and miRNAs. Other analytes are collected (sampled), e.g., by using nasal or saliva swabs[34] or from sweat or urine.[35] NPs or nanoporous/nanostructured materials have been employed as the solid phase for analyte sampling. For example, superparamagnetic beads are a convenient tool for sampling and preconcentration of an analyte,[36] and are discussed in the context of magnetic bead assays (Section 4.1.2).

### 3.2. Affinity Binders

Common sample matrices are complicated environments, in which the analyte constitutes only a minor component. Thus, the analyte detection requires highly specific and selective recognition elements (**Table 2**) such as antibodies that remain the most common biorecognition element in commercial devices.[37] Antibodies, however, are not without problems in terms of production, molecular size, stability, storage, and handling. Therefore, alternative recognition elements have been explored mainly to reduce the price and to improve the stability under ambient conditions. Aptamers and molecularly imprinted polymers (MIPs)[38] are promising alternatives provided that they match the specificity and selectivity of antibody binding. Other bioaffinity binders include peptide mimetics, synthetic receptors based on molecular complexes,[39] or natural receptors for ligand assays.[40] As a unique feature of NP–binder conjugates, they enable using lectins as binders for the detection of cancer-specific protein glycovariants, which are not possible with molecular labels due to the weak affinity of lectins).[41]

#### *3.2.1. Antibodies and Nanobodies*

Antibodies enable specific interactions with high binding constants ($>10^{10}$ $M^{-1}$)[42] and can be routinely produced in large quantities.[43] The high specificity of antibodies is one of the key requirements for the development of assays and sensors.[44,45] Antibodies belong to the superfamily of immunoglobulins (IgG), which play a crucial role in the immune systems of higher animals. Typical IgG antibodies are heterodimers composed of two identical light chains and two identical heavy chains, forming a Y-shaped molecule of roughly 10 nm in diameter with a molecular weight of 150–160 kDa depending on the IgG subclass.

After immunizing an organism with the antigen, numerous clones of plasma cells produce antibodies against different antigenic determinants (epitopes). Such polyclonal antibodies can be prepared relatively easily and tolerate small changes in the nature of the antigen (e.g., denaturation or polymerization), but their affinity is variable, and their production is limited in quantity and requires various purification steps. By contrast, monoclonal antibodies that are derived from an individual plasma cell clone are specific for a single epitope. The preparation of monoclonal antibodies was enabled by the development of hybridoma technology,[46] which is based on the fusion of B-lymphocytes with the immortal myeloma cell line.[46] Alternatively, monoclonal antibodies can be prepared by phage display technology, which is based on presenting recombinant antibody structures on the surface of bacteriophages, followed by testing the interactions with the target antigens.[46] The main advantages of monoclonal antibodies include high specificity, defined biological activity, and the possibility of large-scale production.[37]

The smallest antibody fragment capable of binding antigens is the Fv fragment consisting of one variable domain per light and

**Table 1.** List of selected NP-based detection platforms on the market.

| Company/product | Assay technology | Label | Analyte/performance | Time | Website |
|---|---|---|---|---|---|
| AIDIAN/QuikRead go | Immunoturbidimetry | Latex particles | Clinical analytes | 2 min | www.aidian.eu |
| BioSquare/QuantumPack Easy | LFA | QDs in silica NPs | Viral antigens | 10 min | bio-square.com |
| Clip Health/Clip COVID Rapid Antigen Test | LFA | PLNP (strontium aluminate) | SARS-CoV-2 nucleocapsid/LOD: $0.9 \times 10^2$ $TCID_{50}$ [mL][a)] | 30 min | cliphealth.com/products/covid-19/ |
| Gentian/GCAL | Particle-enhanced turbidimetric immunoassay | Polystyrene NPs | Calprotectin/LOQ: 0.30 mg $L^{-1}$ | 10 min | www.gentian.com |
| Luminex/xMAP | Flow cytometry-based counting | AuNPs (13–20 nm) | Proteins | <2 h | www.luminexcorp.com/magplex-microspheres/ |
| Lumito AB/SCIZYS | Immunohistochemistry imaging | UCNPs (<30–80 nm) | Tissue cancer markers | – | lumito.se/en/products/ |
| MagArray/MagArray System | Magnetoresistance | Superparamagnetic NPs (≈50 nm) | EGFR/10 ng $mL^{-1}$ | 2.5 h | magarray.com |
| Medisensor/aQcare Chlamydia TRF-S | LFA | EuNPs | *Chlamydia trachomatis* antigen/LOD: 0.27 ng $mL^{-1}$ | <30 min | medi-sensor.com/en/aqcare-chlamydia-trf-s_us |
| MIP Discovery/SARS-CoV2-nanoMIP | Thermal resistance | nanoMIP (54–60 nm) | SARS-CoV2-RBD/5 fg $mL^{-1}$ | – | https://mipdiscovery.com/product/covid-19-nanomips-optimized-for-sensors/ |
| OPKO/Claros 1 | Silver enhancement of AuNPs and optical detection | AuNPs | Total PSA/LOQ: 0.1 ng $mL^{-1}$ | 10 min | www.opko.com |
| Quidel/Triage System | LFA | Fluorescent dye-doped latex particles | Clinical analytes | 15 min | www.quidel.com/immunoassays/triage-test-kits |
| Revvity/Ronia | LFA | UCNPs | PIGF | ≈30 min | https://en.novabio.ee/news/meet-ronia |
| Quanterix/SimoA | Optical detection in fL-sized wells | Superparamagnetic beads | Various proteins | – | www.quanterix.com |
| SAFIA Technologies | Flow cytometry-based counting | Fluorescent dye-doped polystyrene NPs | Mycotoxins | | www.safia.tech |
| Siemens Healthineers/Atellica VTLi | Frustrated total internal reflection microscopy | Superparamagnetic NPs | cTnI/LOD: 1.2 ng $L^{-1}$ (plasma) 1.6 ng $L^{-1}$ (whole blood) | 8 min | www.siemens-healthineers.com/de/cardiac/cardiac-systems/atellica-vtli |
| Uniogen/UPCON | LFAs and microtiter plate assays | UCNPs (>100 nm) | CA125/LOD: 5.4 U $mL^{-1}$ | 30 min | uniogen.com/upcon |
| Vazyme/Various test kits | LFA | QDs | Various | 5–15 min | en.vazymemedical.com/Quantum-Dot-Immunofluorescence-Platform-pl3961912.html |

[a)] $TCID_{50}$—median tissue culture infectious dose (virus dilution required to infect 50% of a given cell culture).

heavy chain. Using molecular biology tools, recombinant single-chain Fv (scFv) fragments can be prepared. These can either carry the specificity of the parent antibodies, or scFv fragments with newly designed binding sites can be prepared using protein engineering and searching for gene libraries.[37,47]

In the 1990s, heavy-chain antibodies without light chains were identified in camelids (hcAbs)[48] and cartilaginous fish (IgNAR).[49,50] The main advantage of heavy-chain antibodies compared to conventional ones is the higher stability and smaller size, enabling better accessibility to some epitopes. Furthermore, they can be more easily optimized by phage display techniques because all the binding specificity is provided by a single peptide strand. For immunochemical applications, the recombinant variable domain of hcAb (also called "nanobody") can be obtained and modified for the binding of the target antigen.[51,52] Such antibodies combine high thermal stability with resistance to proteases and the ability to capture epitopes that are not able to react with whole antibodies.[53] The much smaller size is very important for some applications such as Förster resonance energy transfer (FRET),[54] and they can be more easily designed as fusion proteins.

### 3.2.2. Aptamers

Research on alternative recognition elements that are highly specific for a target analyte and chemically stable is focused mainly on aptamers.[55] While antibodies consist of 21 amino acid building blocks, aptamers consist of only four nucleotide building blocks with a typical length of 40 bases, which defines a potential sequence space of $4^{40}$ combinations.[56] It should be

**Table 2.** Overview of affinity binders commonly used for assays and sensing.

| Affinity binder | Material | Advantages | Disadvantages |
|---|---|---|---|
| Polyclonal antibodies | Proteins<br>150–160 kDa | Simple preparation of single batch<br>Tolerance to small changes in antigen<br>Good commercial availability<br>Reasonable price | Limited stability (temperature, proteases)<br>Heterogeneity between batches<br>Increased changes for cross-reactivity as they are specific for the whole target protein rather than a single epitope |
| Monoclonal antibodies | Proteins<br>150–160 kDa | Simple large-scale production<br>High specificity<br>Good commercial availability<br>Reasonable price | Limited stability (temperature, proteases) |
| Cameloid and recombinant antibodies, and nanobodies | Proteins<br>15 kDa | High thermal stability<br>Small size<br>Ease of genetic engineering<br>Possibility to capture epitopes not reacting with whole antibodies | Lower commercial availability than antibodies |
| Nucleic acid aptamers | DNA, RNA<br>40 bases | Possibility of in vitro chemical synthesis<br>Simple large-scale production<br>Higher temperature and chemical stability, possibility of regeneration by heat<br>Small size | Lower affinity than antibodies<br>Challenging preparation for new targets<br>Susceptibility to nucleases |
| Peptide aptamers | Peptides<br>5–20 aa | Possibility of in vitro chemical synthesis<br>Simple large-scale production<br>Higher temperature stability, possibility of regeneration by heat<br>Small size | Challenging preparation for new targets |
| Molecularly imprinted polymers | Polymers | Fully synthetic<br>Excellent physical and chemical stability | Limited access of larger molecules (proteins)<br>Limited specificity<br>Heterogeneity between batches and individual binding sites |

noted that some authors only define recognition elements based on three-dimensionally folded single-stranded DNA or RNA as aptamers,[57] while others classify both nucleic acid- and peptide-based recognition elements as aptamers.[58] Typically, DNA aptamers are chemically more stable, while RNA aptamers are conformationally more flexible and thus possess a larger structural variety.[59]

While both types of nucleic acid aptamers do not differ significantly in terms of specificity or affinity,[60] the difference to the affinities of antibodies can reach several orders of magnitude (nM range for antibodies and μM range for aptamers), which is often not sufficient for the detection of clinically relevant concentrations. In the literature and commercial applications, aptamers are mostly used for a few analytes such as thrombin, cocaine, ATP, and lysozyme, for which well-defined target-binding sequences are known.[61] This repertoire of targets, however, is small compared to the wide variability of commercially available antibodies.

In general, aptamers are used in similar configurations as conventional immunoassays and sensors.[62] Unlike immunoassays, however, aptamer-based assays can be regenerated by using heat for denaturation, which leads to the release of the bound analyte. When the temperature is lowered, the aptamers refold to the functional conformation and can again bind the analyte, which allows for reusing the assay.[63] Alternatively, nucleic acid-based aptamers can be regenerated using proteinase K, which specifically degrades the target proteins but not the aptamer.[62] Aptamers are also more resistant against heat and chemicals than antibodies, but they are susceptible to degradation by nucleases present in cells and body fluids. The degradation stability can be improved by a chemical modification of the nucleotides.[64]

Nucleic acid aptamers allow for an easy and cost efficient in vitro chemical synthesis and they are typically optimized from a large library of oligonucleotides ($\approx 10^{15}$ different structures) by systematic evolution of ligands by exponential enrichment (SELEX). SELEX involves three main steps: 1) binding of the target molecule to the library, 2) elution of the bound oligonucleotides, and 3) amplification by PCR.[65] These steps are repeated 8 to 15 times to obtain an enriched pool of sequences with high affinity and specificity for the target. The enriched sequence with the highest concentration is selected as the potential aptamer.[57] While SELEX typically requires several days or weeks, nonequilibrium capillary electrophoresis of equilibrium mixture (NECEEM)-based partitioning is an alternative procedure without amplification steps that only takes 1 h.[66] The preparation of new aptamers via SELEX or NECEEM, however, is not always successful and can be rather complicated from a practical

point of view. Thus, in future commercial applications, aptamers may not replace antibodies in general, but they may find applications whenever high-affinity aptamers are available.

Peptide aptamers are short constrained amino acid sequences (5–20 amino acids) embedded into a small and stable protein backbone that are identified by the phage display technology.[67,68] The conformational constraint stabilizes the insert loop and enables the aptamer to fold and recognize the target molecules.[67]

#### 3.2.3. Molecularly Imprinted Polymers (MIPs)

MIPs, also called "plastic antibodies," are fully synthetic recognition elements, which are generated by polymerizing their constituent monomers in the presence of a target molecule, which serves as a template.[69] After removing the template, cavities with shape, size, functionality, and spatial arrangement complementary to the target molecule are formed in the polymer.[70] As the most stable type of recognition element, MIPs bind their targets even after treatment with strong acids or bases, organic solvents, or high temperatures.[71,72] Compared to antibodies or aptamers, MIPs are nevertheless much less common in assays and sensors and respective commercial products because there is a large heterogeneity between individual binding sites,[73,74] which typically leads to more cross-reactivity and nonspecific binding.[75] The hydrophobic and highly cross-linked structure of MIPs also restricts access of larger molecules like proteins to the imprinted sites, which may further compromise the assay performance.

As a successful example of commercialized MIP applications, the British company MIP discovery (mipdiscovery.com) imprinted nanoMIPs against a part of the receptor binding domain (RBD) of the viral spike protein. Such SARS-CoV-2 nanoMIPs were immobilized on an electrode surface to measure the thermal resistance at the interface between the electrode surface and the aqueous sample matrix (thermal resistor sensor platform).[76]

### 3.3. Signal Generation Elements

Even though there are label-free biosensing approaches,[77] most bioaffinity assays employ labels such as enzymes or fluorescent dyes for the sensitive analyte detection. More recently, the progress in nanotechnology has led to the development of new NP-based labels (**Table 3**) that are detected optically, e.g., by light absorption (colorimetry, nanocatalysts that produce a chromophore), luminescence (fluorescence, electrochemiluminescence), scattering (turbidometry, nephelometry, surface-enhanced Raman spectroscopy (SERS)), but there are also examples of electrochemical detection and the use of superparamagnetic NPs as labels. Most commercial applications are currently based on AuNPs for visually readable LFAs and latex NPs for qualitative agglutination and quantitative turbidimetric/nephelometric assays.

While optical labels are most common and will be further explained in the next section, other assays combine different methods such as optomagnetic detection or magnetoresistance.[45,78] For example, MagArrays are based on measuring the change of magnetoresistance when superparamagnetic beads come close to magnetoresistive multilayer thin film (sensor surface).[79,80] Mag Arrays have mainly been used to study one specific interaction between an immobilized molecule and an NP-labeled molecule.

#### 3.3.1. Gold Nanoparticles (AuNPs)

AuNPs are one of the most widely used labels in bioaffinity assays and sensors. Due to their remarkable optical, chemical, catalytic, and electrical properties, AuNPs have found applications especially in LFAs, colorimetric assays, plasmonic sensing, and electrochemistry.[81,82] Their specific properties—and thus also applications—are size and shape dependent. In the case of small AuNPs (colloids below 100 nm), the dispersions have an intense red color, which changes to yellow in the case of larger particles.[83] Localized surface plasmon resonance (LSPR) leads to oscillations of the free electrons of AuNPs, which is resonant with a specific wavelength of light.[84]

AuNPs are typically synthesized by the method of Turkevich et al.,[85] with further improvements by Frens.[86] Gold salts or tetrachloroauric acid ($HAuCl_4$) are chemically reduced by citrate, leading to monodisperse spherical NPs. The shape and size of AuNPs can be modified by changing reagent concentrations, reducing agents, or surfactants.[87] Numerous shapes of AuNPs have been reported over the years, including nanorods, nanostars, core–shell structures, nanoclusters, and irregularly shaped AuNPs.[45] AuNPs can also be combined with silver enhancement.[88] The surface of AuNPs can then be modified with biomolecules, such as antibodies, DNA, or enzymes, to generate target-specific nanoprobes for various analytes.[89] The bioconjugation reactions typically exploit the strong affinity of mercapto[90] or amino[91] groups to gold, which form self-assembled monolayers on the surface of AuNPs. The biomolecules retain their activity after immobilization on AuNPs and the bioconjugates are well biocompatible.

The high molar extinction coefficients and significant color changes upon aggregation have led to the development of numerous colorimetric[92] and LFAs.[93,94] The ability to quench the fluorescence signals due to energy transfer between fluorophores and AuNPs enabled applications in fluorescence assays,[95] the electrochemical properties of AuNPs are utilizable in impedance biosensors,[96] their catalytic activity can be exploited to amplify the optical or electrochemical signals,[88] and their plasmonic properties find applications in LSPR assays[97] and amplify the performance of surface plasmon resonance biosensors.[98] Finally, the low toxicity of AuNPs[96] enabled their applications in in vivo diagnostics and imaging.[99] Overall, AuNPs are fully established labels with high stability and well-characterized bioconjugation procedures, making them the first choice in numerous bioaffinity tests.

#### 3.3.2. Dye-Doped (Silica/Polymer/Latex) NPs

Dye-doped micro- and nanobeads became widespread in recent years. A bead typically consists of thousands of fluorophore molecules encapsulated in a polymer (e.g., polystyrene) or silica matrix, and thus is much brighter than a conventional fluorophore label.[100] It should be expected that $n$ fluorophore molecules present in the polymer matrix result in an $n$-fold

**Table 3.** Overview of NPs commonly used as labels for assays and sensing.

| Signal generation element | Material | Mechanism | Specific advantages |
|---|---|---|---|
| Noble metal NPs | Gold, silver | Light scattering<br>Localized surface plasmon resonance<br>Fluorescence quenching<br>Catalytic activity | Naked-eye readout<br>Useful in wide range of readout methods<br>Well-optimized bioconjugation methods<br>Low toxicity |
| Latex NPs | Latex | Increased light scattering upon agglutination | Simple application |
| Dye-doped NPs | Polymer + dye | Fluorescence | High brightness<br>Good photostability<br>Low toxicity<br>Doping with multiple dyes enables ratiometric sensing |
| Lanthanide chelate-doped nanoparticles (LnNPs) | Polymer + chelated lanthanide | Fluorescence | High brightness<br>Time-gated detection facilitating separation from background<br>Large Stokes shifts |
| Quantum dots (QDs) | Semiconductors | Quantum confinement<br>Fluorescence | Tunable emission<br>Narrow and symmetric emission bands<br>High quantum yields<br>Broad excitation spectra |
| Polymer dots (Pdots) | Polymers with semiconductor properties | Fluorescence | Photostability<br>Biocompatibility<br>Tunable optical properties |
| Photon-upconversion nanoparticles (UCNPs) | Rare earth salts | Photon-upconversion luminescence | Background-free detection<br>Tunable emission<br>Large anti-Stokes shifts<br>Excellent photostability<br>Low toxicity |
| Persistent luminescence nanoparticles (PLNPs) | Inorganic materials | Fluorescence<br>Phosphorescence | Luminescence measurement without continuous illumination<br>Avoids autofluorescence and light scattering from biological materials |
| Surface-enhanced Raman spectroscopy (SERS) | Au or Ag NPs + organic Raman label molecule + protective shell | Raman scattering | Narrow spectroscopic signatures<br>High degree of multiplexing |

stronger signal as compared to a single fluorophore label. During the readout, however, the photon flux may not be sufficient to concurrently excite all of *n* fluorophores clustered in a very small volume and the fluorescence of molecular fluorophores in close proximity is typically quenched. The quenching can be avoided by sophisticated fluorophore arrangements in the matrix,[101] or if suitable NPs such as liposomes are dissolved before the readout to release the fluorophores.[102]

Additionally, the NPs can be doped with multiple dyes, enabling ratiometric sensing.[103] Other advantages of dye-doped beads include a good photostability and low toxicity.[104] There are also commercial (nano)particles, which contain FRET pairs to increases the Stokes shift such as TransFluoSpheres originally developed by Molecular Probes ($\lambda_{exc}$ 488 nm; $\lambda_{em}$ 514 nm) or even further in the red spectrum as the Quidel Triage System ($\lambda_{exc}$ 670 nm; $\lambda_{em}$ 760 nm).[105] The larger Stokes shift enables a better discrimination from autofluorescence.

### *3.3.3. Lanthanide Chelate-Doped NPs (LnNPs)*

Organic chelates of certain lanthanide ions, especially europium ($Eu^{3+}$), display luminescent properties that are highly desirable for labels in diagnostic assays. In particular, lanthanide complexes exhibit long-lived luminescence with large Stokes shifts. The slow luminescence decay allows time-gated or time-resolved detection, facilitating the separation of the specific emission signals from the background fluorescence.[106] The lanthanides are typically chelated with antenna dyes that absorb UV excitation light and transfer it to the lanthanide. To further enhance the luminescence yields, lanthanide complexes are often

assembled into a polymer matrix, forming LnNPs.[107–109] Depending on the particular chelating structures, LnNPs incorporate thousands of luminescent chelates in a protective hydrophobic shell, resulting in chemical stability and bright luminescence.[110] It should be noted that lanthanide complexes enclosed in LnNPs exert a much weaker mutual quenching effect than organic fluorophores in dye-doped NPs. Therefore, EuNPs provide the potential to strongly improve the sensitivity of immunoassays, especially LFAs.[111,112] Several companies such as Medisensor from Korea provide EuNPs as labels for the detection of *Chlamydia trachomatis* antigens and provide their own dedicated LFA readers for PoC applications.[113]

#### 3.3.4. Quantum Dots (QDs)

QDs are one of the most frequently used labels because they are optically very attractive small-size labels. QDs are semiconductor nanocrystals that show a quantum confinement effect depending on their size—typical 1–10 nm in diameter —[114] and material composition.[115] QDs are typically composed of group II–VI (e.g., CdTe and CdSe) and III–V (e.g., InP) semiconductors. Also core–shell structures, with a shell based on wider bandgap semiconductor material (e.g., ZnS), are widely employed to reduce the toxicity and improve the luminescence properties.[116] By optimizing the chemical composition and size of QDs, their emission wavelength can be continuously tuned from 380 to 2000 nm.[117,118] Other advantages of QDs compared to conventional organic fluorophores[119] include narrow and symmetric emission bands (full-width-at-half maximum 25–35 nm), high quantum yields (up to 89% at room temperature),[120] and broad excitation spectra.[121]

QDs are typically synthesized in organic solvents at high temperatures.[122] To enable the transfer of such hydrophobic QDs to aqueous solutions, the hydrophobic ligand layer on the surface must be exchanged with a more hydrophilic material. The two main approaches include ligand exchange and encapsulation with an amphiphilic polymer.[123,124] Hydrophilic ligands with mercapto groups are typically used for ligand exchange due to their high binding affinity to the QD surface.[125] Bioconjugates of QDs and recognition molecules are highly stable and easily detectable, which renders them useful as sensitive labels for various formats of luminescence assays,[126–128] electrochemiluminescence sensing,[129] and bioimaging.[130,131] In addition, when QDs of different emission colors are embedded in polymeric microbeads at precisely controlled ratios, labels enabling multiplexed color encoding can be prepared.[132]

In commercial assay platforms, QDs may be limited by a complex surface chemistry and the highly toxic cadmium in an otherwise favorable chemical composition.[133] While the amount of cadmium from QDs per single test is typically small enough (micrograms) to meet RoHS requirements, the manufacturers would have to handle larger quantities of cadmium-based materials, which should be avoided according to the European directives on safety and health at work unless there are no alternatives.

The Korean company BioSquare has commercialized QuantumPack, which uses silica NPs with QDs in an outer shell as fluorescent labels for LFAs, and a dedicated QDITS PoC immunoassay analyzer for the readout. The QD-based LFA was more sensitive than the Sofia Influenza A + B fluorescence immunoassay (Quidel, USA).[134]

#### 3.3.5. Conjugated Polymer Nanoparticles (CPNPs) and Semiconductor Polymer Dots (Pdots)

Conjugated polymers consist of large $\pi$-conjugated polymer backbones with a delocalized electronic structure reminiscent of inorganic semiconductor materials. Their optoelectronic properties including light-harvesting, light-amplification, and high photostability render them useful for a wide range of applications such as light-emitting diodes, photovoltaic cells, and field effect transistors.[135]

CPNPs are a relatively new alternative signaling element for assays, sensors, and imaging applications because they are strongly luminescent and their absorption and emission is tunable depending on the molecular weight and polymer chain interactions.[136,137] Various approaches for the development of water-dispersible CPNPs have been proposed, but their preparation is rather complicated.[138] The main progress in assay and sensor applications was realized after the development of water-dispersible CPNPs. The functionalization of CPNs with specific recognition elements imparts a good ability for target recognition and imaging in vitro and in vivo.[135]

Semiconducting polymer dots (Pdots) represent a special type of small CPNPs below 30 nm in diameter, preferably in the range of 5–20 nm. Pdots are well-suited for biological analysis and imaging because they are small and very bright.[139] Pdots have found applications as labels in LFAs, e.g., for the detection of PSA,[140,141] carcinoembryonic antigen or cytokeratin 19 fragment.[142] Pdots are an interesting alternative label for LFAs, but such assays have not been commercialized, yet.

#### 3.3.6. Photon-Upconversion Nanoparticles (UCNPs)

Lanthanide-doped UCNPs absorb two or more photons of low energy near-infrared light and emit one photon of higher energy (anti-Stokes emission).[143] Compared to two-photon excitation or second harmonic generation, much lower energy densities are sufficient for the excitation of UCNPs. One of the most efficient UCNPs are composed of a crystalline host matrix (typically $NaYF_4$) doped with low concentrations of the sensitizer $Yb^{3+}$ and the activators $Er^{3+}$ or $Tm^{3+}$.[144] New synthesis methods have yielded UCNPs with better photoluminescence quantum yields.[145] As UCNPs are typically synthesized in hydrophobic solvents, their surface needs to be modified, e.g., by a silica shell or by ligand exchange reactions, to enable biological applications.[16] For example, heterobifunctional ligands containing phosphonate or carboxylate groups coordinate at one end to surface lanthanide ions and the other end is available for subsequent bioconjugation steps.[146]

Unlike other luminescent labels, the excitation of UCNPs completely avoids background signals due to autofluorescence from any solid-phase material employed in bioaffinity assays. Consequently, relatively simple readout devices for the specific detection of UCNP labels enable an extremely high analytical

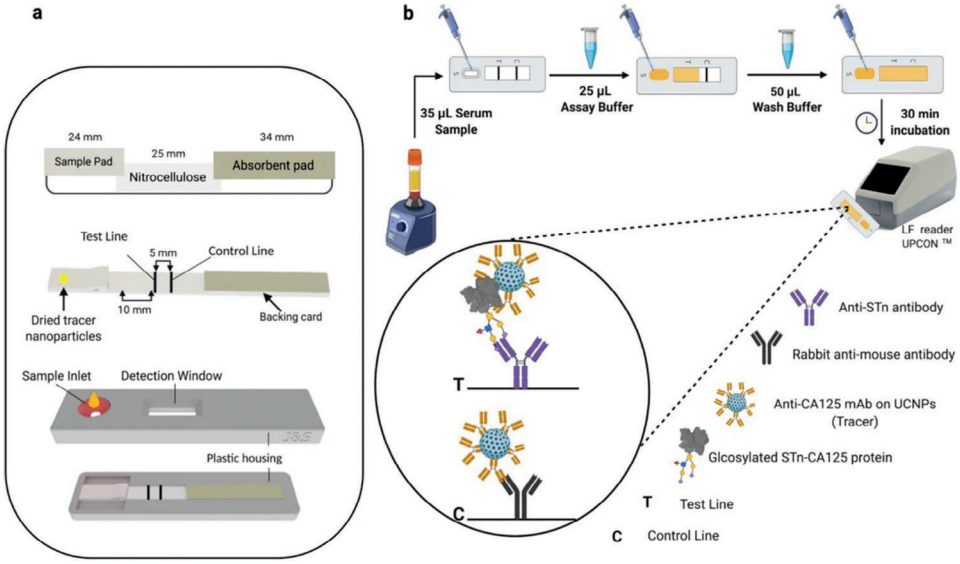


**Figure 2.** a) Illustration of LFA strips for the detection of CA125. The test strip consists of a sample pad, nitrocellulose membrane, and an absorbent pad. The sample pad ensures an even flow of the sample and the UCNP label to the nitrocellulose membrane. b) Experimental workflow of the LFA. Reproduced under the terms of the Creative Commons Attribution 4.0 International License from.[155] Copyright 2020, the authors.

sensitivity, which is a significant competitive advantage in commercial applications.[147,148] The availability of less complex readout devices is particularly important when the platform is intended for PoC.[149,150] Furthermore, the large anti-Stokes shifts of UCNPs enable an easy separation of the excitation and detection channels, they are completely photostable, and their emission wavelength can be tuned, allowing for signal multiplexing.[151] Due to this broad range of advantages, UCNPs have found numerous applications in microtiter plate-based assays,[152] LFAs (**Figure 2**),[153–156] immunomagnetic assays,[157,158] as well as bioimaging.[146,159]

The company Orasure pioneered the commercial production of upconversion labels for bioaffinity assays.[160] While many research groups still synthesize their own UCNP labels, the Finish company Uniogen currently provides certified UNCP-labels that are consistent in size and brightness, along with readers for microtiter plates and LFA strips. More recently, the new company Revvity commercialized the Ronia reader for UCNP-based LFAs. For immunohistochemistry, the Swedish company Lumito is developing the SCIZYS reader to the market for wide-field upconversion whole slide imaging with cellular resolution.[159,161] Compared to the detection of organic fluorophores or enzyme-generated chromogenic products, imaging of UCNP labels strongly improves the sensitivity and dynamic range,[162] which is necessary to monitor differences in protein expression that may span four orders of magnitude.

### 3.3.7. Persistent Luminescence Nanoparticles (PLNPs)

PLNPs emit long-lasting luminescence after stopping the excitation. Measuring luminescence signals without continuous external illumination avoids interferences of autofluorescence and light scattering from biological materials without the need for expensive instrumentation with time-resolved capabilities.[163] Such optical properties have enabled the use of PLNPs in biosensing and imaging applications,[164] as well as in theranostics.[165]

PLNPs based on $Eu^{2+}$- and $Dy^{3+}$-doped $Ca_{1.86}Mg_{0.14}ZnSi_2O_7$ were used for the detection of $\alpha$-fetoprotein (AFP). PLNPs were coated with polyethyleneimine and AuNPs were coated with anti-AFP antibody. When both components were combined, they adhered to each other and the close proximity of PLNP and AuNP led to FRET, which quenched the luminescence. Binding of AFP to the antibody-coated AuNPs released the AuNPs from the PLNP surface and recovered the luminescence signal. This competitive assay resulted in an LOD of 0.41 ng $mL^{-1}$.[166]

Additionally, wet milling of phosphorescent strontium aluminate ($SrAl_2O_4$) powder yielded PLNPs that were then encapsulated in silica incorporating an aldehyde silane.[167] Then, an amine-poly(ethylene glycol)-carboxyl linker was attached to facilitate the covalent binding of proteins. The attachment of neutravidin enabled the use of the PLNPs as a sensitive immunoassay label. Similarly, the US company Clip Health employs $SrAl_2O_4$ as a label for their Covid-19 Rapid Antigen Test (LFA) that is read out by the Clip Core device, a hand-held and smartphone-connected fluorescence reader for LFA cartridges.

### 3.3.8. Surface-Enhanced Raman Spectroscopy (SERS) Tags

SERS is a light scattering method that has attracted wide interest in recent years as a detection method for clinical biomarkers.[168] As Rayleigh scattering and autofluorescence is many orders of magnitude stronger than Raman scattering, it is typically challenging to specifically detect the Raman signal above the background signal. Noble metal nanostructures such as metal colloids, roughened metal surfaces, nanosphere self-assemblies,

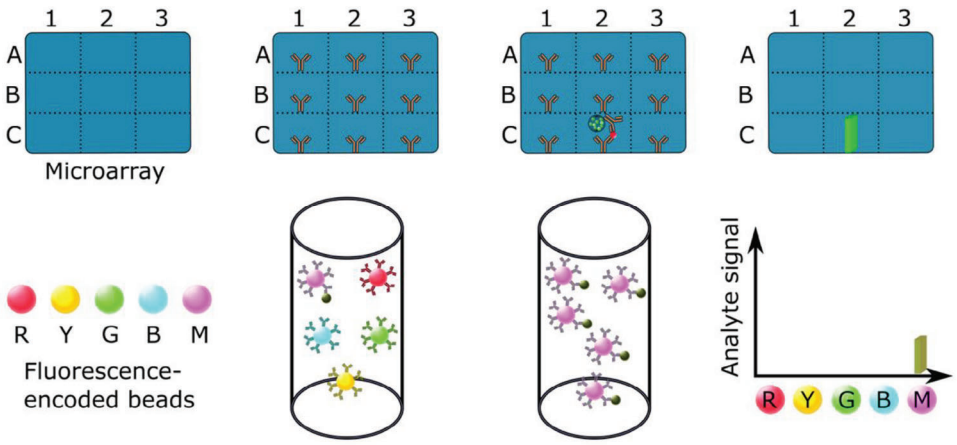


**Figure 3.** (Top) Spatial multiplexing on planar arrays can be implemented based on many different types of labels while (bottom) suspension arrays typically rely on fluorescence-encoded beads.

template-directed deposits, and numerous core–shell NPs, however, provide the potential to enhance Raman signals by a factor of $10^7$ to $10^{14}$ which is suitable for the design of sensitive bioaffinity assays.[121]

SERS has been used for the direct detection of food-borne pathogens.[169] For example, *Staphyloccocus aureus* and *Listeria monocytogenes* were first captured using wheat germ agglutinin (a lectin) on magnetic iron oxide NPs. Subsequently, AuNPs linked to species-specific aptamers served as Raman tags to distinguish between these bacteria.[170] In other applications, SERS labels were used as detection elements in LFAs. For example, serum IgG and IgM against SARS-CoV2 spike protein were captured separately in two test-zones and detected using Raman tags consisting of spike protein conjugated to Ag(shell)/$SiO_2$(core)/5,5′-dithiobis-(2-nitrobenzoic acid).[171] The readout by a portable B&W Tek i-Raman Plus BWS465 spectrometer achieved a 1000-fold lower LOD compared to standard colloidal gold detection. The preparation and application of well-defined and reproducible noble metal surfaces that are required to enhance the Raman signal, however, is a high hurdle for SERS-based techniques on the way from the research laboratory into routine clinical diagnostics (**Figure 3**).

### 3.4. Multiplexing

In many applications, there is a strong need to detect several analytes in parallel. The first approach for multiplexing is based on positional addressing (spatial multiplexing), where multiple capture elements are immobilized on different segments of the sensing array (**Figure 4**). In the simplest case, different wells of microtiter plates or several test lines in LFA test strips represent these segments.[172] The degree of multiplexing can be strongly upscaled by using miniaturized arrays of thousands of spots in the case of protein or DNA arrays (e.g., gene chips from Affymetrix).[173]

The second approach exploits labels (organic dyes or NPs) that display distinct detection signatures such as the emission color to distinguish between several analytes.[174] The number of analytes detectable in parallel, however, is limited by overlapping emission bands of fluorescent dyes.[175] Dye-doped nano- and microparticles (beads) are interesting candidates for color-coding because different combinations of fluorescent dyes can be assembled into one NP in different ratios such that color coding is based on wavelength and intensities, which strongly enhances the encoding capacity. Bead-encoded arrays can be read out

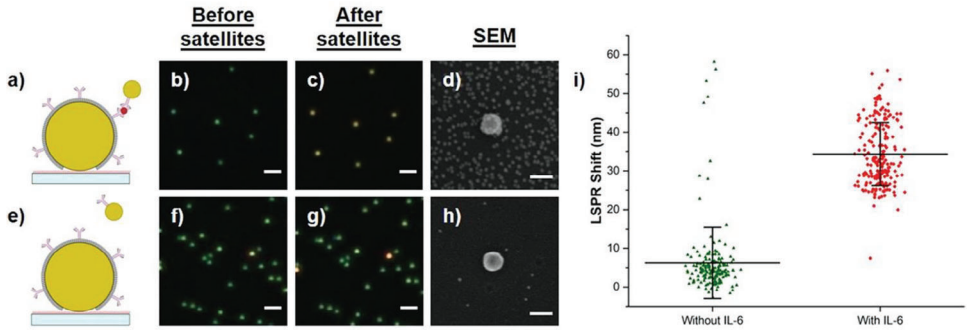


**Figure 4.** Digital immunoassay based on the detection of single AuNPs by dark-field microscopy. Assay scheme a) in the presence of IL-6 and e) without IL-6. In the presence of 4.76 nM of IL-6, the color changes from b) green to c) orange after incubation with the satellites. f,g) Without IL-6, the color does not change. Scale bar: 2 µm. SEM images show d) 10 nm satellites bound to a AuNP due to IL-6 binding, while h) the AuNP carries no satellites in the absence of IL-6. Scale bar: 100 nm. i) LSPR shifts of AuNPs for the control ($n = 176$) and test ($n = 204$). The mean red shifts are 6.2 nm without IL-6 and 34.3 nm with IL-6. Reproduced with permission.[186] Copyright 2018, Elsevier.

simultaneously (randomly ordered arrays) or read one-by-one (suspension arrays) but typically require more sophisticated readout schemes than spatial encoding.[176] Other encoding strategies have been developed based on the multiple emission wavelengths and lifetimes of lanthanides.[151,177]

The US company Luminex offers multiplex immunoassays using antibody-coated magnetic microparticles (beads) instead of an antibody-coated microtiter plates to capture the analyte.[158] The beads carry up to 100 unique fluorescence codes consisting of different ratios of two long-wavelength fluorophores. In this suspension array, each analyte-specific bead is identified one-by-one by its unique code with high throughput using a dedicated flow cytometer (xMAP).[178]

Similarly, the German company SAFIA Technologies employs fluorescence-encoded beads for a competitive suspension immunoassay. The bead surface is covered with the analyte, and a specific antibody either binds to the surface-bound analyte or to the free analyte in solution. No washing steps are required because the flow cytometer can distinguish between free and bead-bound fluorophores, which renders the measurements faster and easier compared to microtiter plate immunoassays.[179]

### 3.5. Digital Assays

Digital bioaffinity assays require the highest sensitivity of label detection because each label must be detected and counted individually to indicate the presence of a distinct single analyte molecule as recently discussed.[15,180] The US company Quanterix uses magnetic beads as a capture surface and the enzymatic generation of a fluorescent product for their single molecule array (SiMoA) platform.[181] In this enzyme-linked immunosorbent assay (ELISA)-type detection scheme, it is essential to suppress product diffusion through femtoliter-sized arrays in order to assign a signal to a single analyte molecule only.[182] Compared to enzymes, however, extremely bright NPs (such as dye-doped polymers) or NPs that can be detected without optical background interference (such as UCNPs) seem to be more suitable detection labels because there is no need to prevent product diffusion after such an NP label has bound to a single analyte molecule.

For example, individual immune complexes labeled with a single UCNP were counted in a conventional microtiter plate format by fluorescence microscopy for the detection of PSA,[183,184] cardiac troponin,[152] and SARS-CoV-2.[185] Plasmonic AuNPs in combination with dark-field microscopy were used for the digital detection of interleukin-6 (Figure 4).[186] Other digital NP-based immunoassays have been implemented by laser heating of AuNPs that generated transient vapor nanobubbles for the digital detection of viruses.[187]

The SiMoA platform, however, continues to be the most successful digital immunoassay on the market. This underlines the fact that the label brightness and the optical signal-to-background ratio are only two among many assay parameters that determine the overall assay performance. In the case of an ultrasensitive detection using digital assays, nonspecific binding of the labels becomes increasingly problematic and, here, the molecular labels seem to have an advantage over larger NP labels.

## 4. From Laboratory Instruments to PoC Devices

We can broadly distinguish between laboratory-based methods and PoC tests, and there is a constant need to turn the instrumental methods into hand-held devices for PoC diagnostics. Liquid chromatography coupled to mass spectrometry typically enables the most sensitive detection of various analytes because they are not limited by the affinity of antibodies or other ligands. Bioaffinity assays, however, play a dominant role not only in PoC tests but also in clinical diagnostics for several reasons: 1) they are relatively easy to perform, 2) they are more easily amenable to mass screening in routine diagnostics, 3) the detection instruments are robust during routine operation, and 4) much cheaper than high-end mass spectrometers. For these reasons, instruments for optical or electrochemical bioaffinity assays can be much more easily converted into hand-held devices compared to mass spectrometers. Many recent commercial PoC platforms and those currently in development are based on microfluidic test cartridges,[188] where the assay is run with minimal sample and reagent volumes. The detection of analytes in such small sample volumes typically requires a stronger signal generation than available from conventional optical labels.

Conventional heterogeneous assays such as microtiter plate immunoassays are sensitive but require relatively long incubation times and several washing steps, which are typically carried out in laboratory conditions. By contrast, homogeneous immunoassays exploit a change in the label signal upon analyte binding to an immunoreagent and require neither solid phases nor washing steps. Homogeneous assays are commonly faster to perform but less sensitive than heterogeneous assays.[189] The type of analyte determines which type of detection format should be employed. For example, sandwich immunoassays are the method of choice for protein markers, which are large enough for binding two antibodies simultaneously, while hormones and chemical warfare agents are relatively small molecules that require competitive assay formats (**Figure 5**).

### 4.1. Solid Phase (Heterogeneous) Immunoassays

Microtiter plates, LFA strips and magnetic beads are typical solid phases for immunoassays[190] that have been used for the analysis of protein biomarkers, other clinically relevant analytes and increasingly also for various trace contaminants in food control and environmental protection.[45] NP-based labels for the readout of solid phase immunoassays can be divided roughly into two categories: (a) plasmonic NPs, such as AuNPs that enable a visual detection for the readout of LFAs, and (b) luminescent NPs that are mainly employed for the readout of microtiter plate assays, but typically require more demanding detection instruments. Depending on the type of luminescent NP, they offer improved luminescence efficiencies, long luminescence lifetimes, large Stokes shifts, narrow emission bands, and high resistance to photobleaching.[15]

#### *4.1.1. Microtiter Plate Assays*

In a typical heterogeneous sandwich assay, an analyte-capturing ligand, typically an antibody, is immobilized on a solid phase, followed by a blocking step, sample application, and the addition of

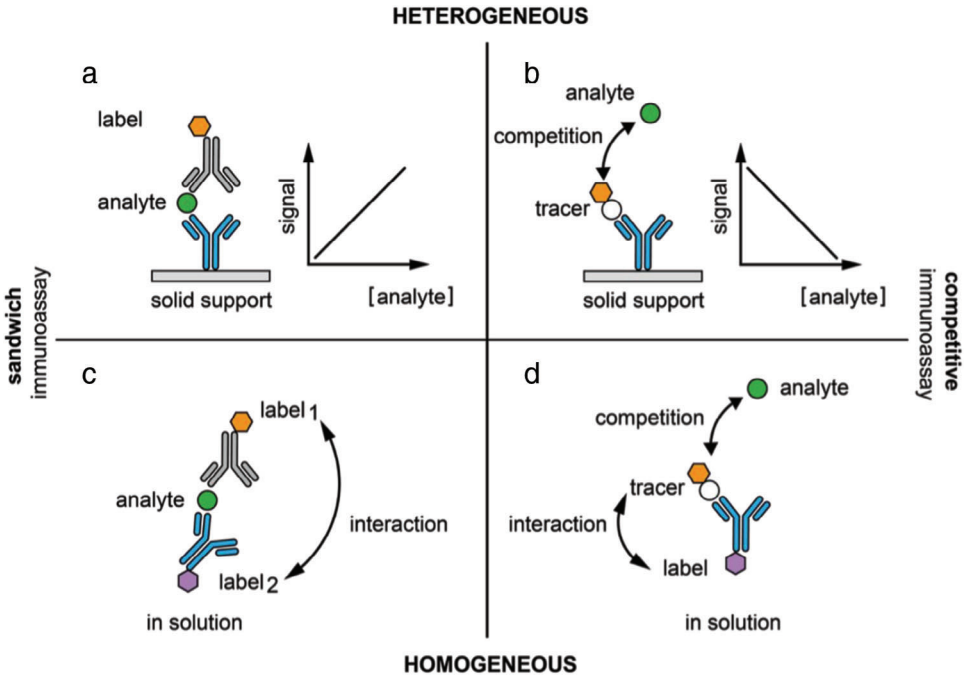


**Figure 5.** Schemes of a) a noncompetitive, heterogeneous immunoassay using a pair of capture (blue) and labeled detection (gray) Ab and b) a competitive immunoassay using only one Ab and a labeled tracer (orange–white) that competes with an analyte (green) for the antibody binding sites. Each assay shows a distinct signal response with increasing analyte concentrations. Homogeneous immunoassays can also be implemented in c) a noncompetitive and d) a competitive assay format, but require a change in the signal response of the labels upon analyte binding.

at least one reagent containing a detectable label to measure the solid phase-bound analyte. Additionally, ample washing steps are employed to remove excess reagents. The washing steps are crucial to reduce the background signal of solid phase immunoassays and are a major reason for the higher sensitivity compared to homogeneous assays. Enzymes are the most widely used labels for immunosorbent assays, and the ELISA is considered the gold standard among diagnostic assays. Other conventional labels include radioisotopes and organic fluorophores, but in general most labeling strategies are applicable to microtiter plate assays.[190]

#### 4.1.2. Magnetic-Bead Assays

Some materials such as magnetite or maghemite are superparamagnetic on the nanoscale (<100 nm in diameter) and move toward an external magnet without magnetically affecting each other. Superparamagnetic capture beads, however, typically are a few micrometers in diameter, which confer a larger surface area for capturing more analyte molecules compared to NPs, but also afford better binding kinetics compared to a planar surface.[190] Therefore, many small superparamagnetic NPs are enclosed in a polymer matrix of a microparticle (bead).

Protocols for bead assays are in principle very similar as protocols for microtiter plate assays and similar labeling strategies can be used. Upon conjugation with specific affinity binders, magnetic beads specifically capture the analyte from the sample. The magnetic separation steps enable in principle more efficient washing and separation steps, which reduce matrix effects and provide the opportunity for analyte preconcentration. The application of magnetic beads dates back to 1970, with their first application in affinity chromatography.[191] Since then, various types and sizes of magnetic beads have found applications in bioanalytical chemistry. Superparamagnetic beads are commercially available from several companies, such as Invitrogen (Dynabeads) or Agilent (Lodestars), and found applications in fully commercialized bioanalytical systems from Quanterix (SimoA)[181] and Luminex.[178]

The German company Siemens Healthineers introduced Atellica VTLi for the detection of cardiac troponin I (cTnI) from a finger prick blood sample (**Figure 6**). Antibody-coated superparamagnetic NPs capture cTnI from the blood sample. Then, a magnet draws the superparamagnetic NPs to a sensor surface coated with a second anti-cTnI antibody to form a sandwich complex. NPs without cTnI are removed from the sensor surface by applying magnetic forces in the opposite direction. For the readout via frustrated total internal reflection microscopy, an inexpensive collimated 625 nm LED illuminates the sensor surface in the total reflection angle. The evanescent field is absorbed and scattered by bound NPs, which causes an intensity decrease in the reflected light that is detected by a CCD camera.[192] Due to the small dimensions and short analysis time, the device enables PoC diagnosis of myocardial infarction.

#### 4.1.3. Lateral Flow Assays (LFAs)

LFAs represent a simple PoC test format, where the flow of a small sample volume deposited on an application pad is driven

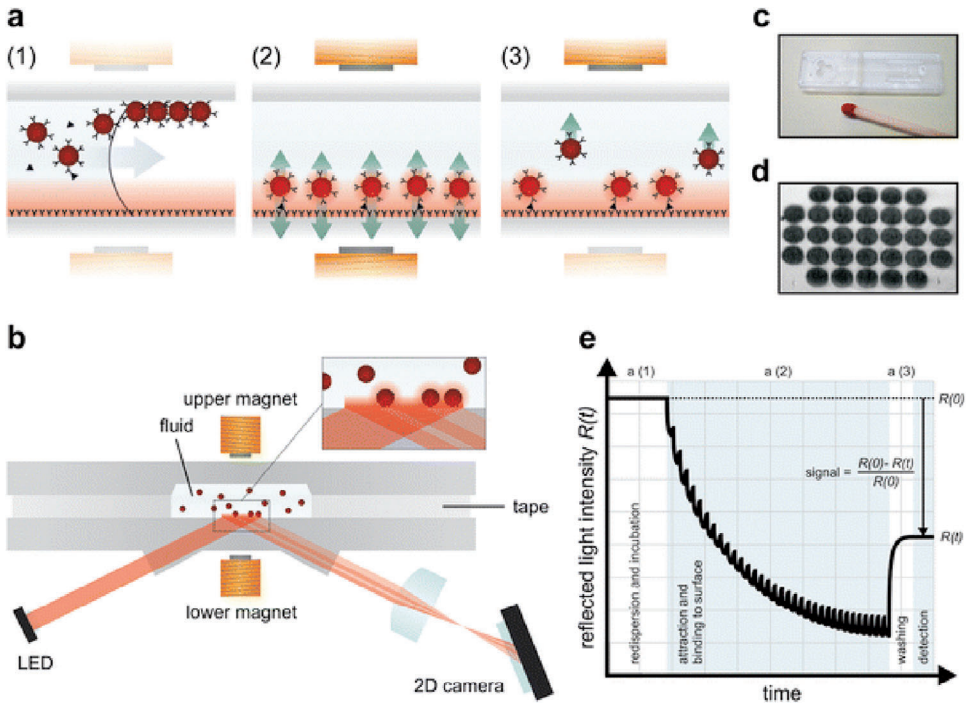


**Figure 6.** Optomagnetic immunosensor using actuated magnetic NPs. a) Scheme of the reaction chamber showing (a1) how the chamber is filled, NP redispersion, and analyte capture, (a2) actuation of the NPs during surface binding, and (a3) magnetic removal of excess NPs from the sensing surface. b) Fluid microchamber with electromagnets and detection optics. Frustrated total internal reflection (f-TIR) allows for measuring the light intensity reflected from the sensor surface, which depends on the bound NP concentration. c) Picture of a disposable cartridge. d) f-TIR image of magnetic NPs bound to 31 antibody capture spots on the sensor surface. e) Real-time signal change on a single capture spot with assay phases indicated as a1–a3. Reproduced with permission.[192] Copyright 2009, Royal Society of Chemistry.

by capillary forces through a nitrocellulose membrane along with immunoreagents and detection labels (**Figure 7**). The presence of the analyte is detected on the antibody capture zone (test line) and a second label detection zone serves as a flow control. Standard LFAs typically rely on light-scattering AuNPs (colloids), but several manufacturers also employ colored latex NPs.[193] Both types of labels can be detected by the naked eye without any instrumental help and thus provide a cost-efficient solution for home testing.[194] Additionally, the assay performance is fast (a few minutes) and easy (the test kit contains all required materials that are cheap and disposable).

After four decades of development and commercialization, the LFA market has grown to an estimated 8.4 billion USD in 2022 and is projected to reach $13.4 billion by 2030.[196] Major

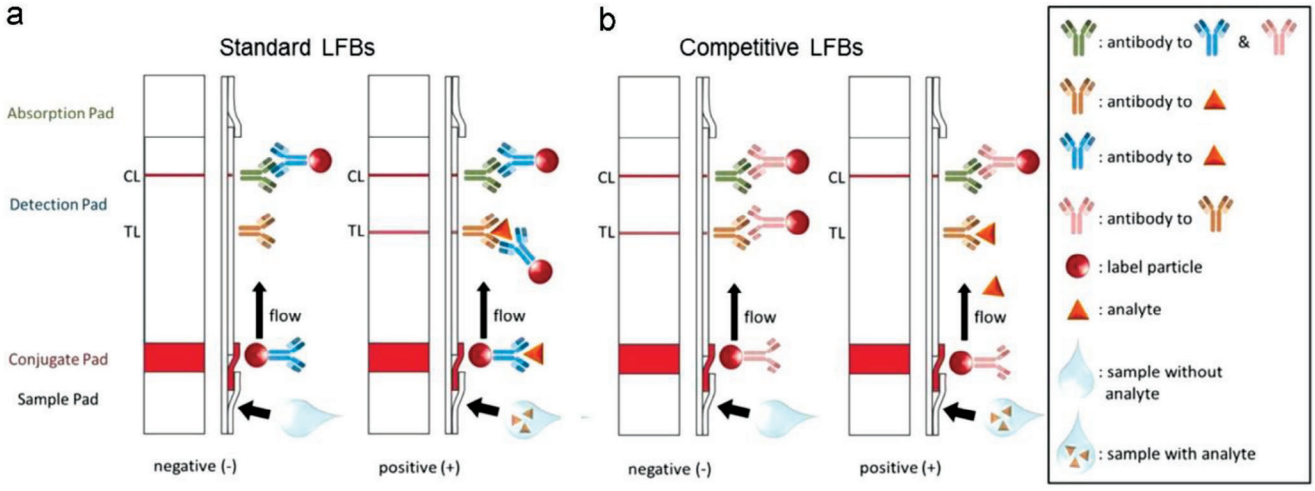


**Figure 7.** Flow of analyte and NP label in a) standard and b) competitive LFAs (TL: test line; CL: control line). Reproduced with permission.[195] Copyright 2015, Elsevier.

companies in the LFA market are Abbott Laboratories (USA), F. Hoffmann-La Roche AG[197] (Switzerland), Danaher Corporation (USA), Siemens AG (Germany), Becton, Dickinson and Company (USA), bioMérieux SA (France), Bio-Rad Laboratories, Inc. (USA), Thermo Fisher Scientific Inc. (USA), QIAGEN N.V. (The Netherlands), and PerkinElmer, Inc. (USA). AuNPs (colloidal gold) remain the most popular labels in the literature as well as in practice.[198]

While pregnancy tests have historically been one of the first and for a long time the most successful LFA on the market,[94] the onset of the Covid-19 pandemic brought a strong impulse for PoC testing as a screening tool to keep the spread of SARS-CoV-2 under control—either in the form of antibody or antigen tests.[199] The development of novel LFAs and their commercialization was further facilitated by the loosened (otherwise very strict) legislative requirements for IVD tests due to the urgent public health emergency. The emergency use authorization (EUA) regulation was adopted by the US Food and Drug Administration and respective organizations in other countries. Over-the-counter rapid tests for home testing thus became a staple in everyday life[200] and have clearly demonstrated their potential to keep the Covid-19 pandemic under control.[194]

Easily available LFAs, which are based on recognition of SARS-CoV-2 antigen from nasopharyngeal samples, were specific, but did not fully match the extreme sensitivity of nucleic acid amplification tests.[201] Although they failed to detect many asymptomatic and presymptomatic infections, the low price as well as an easy and rapid test procedure with visual readout enabled cost-efficient, widespread and frequent mass testing at home or at school, which have assisted in the efforts to counter the spikes of Covid-19 infections.[202] LFA testing has also found many other—not as obvious—applications in the diagnosis of infectious and cardiac diseases, testing of drug abuse, in veterinary medicine, agriculture, environmental monitoring, biological warfare agent detection, and food and feed security.[198]

Even though the analytical sensitivity using a visual readout may not be adequate for all applications—in particular not for quantitative detection—and home testing may be more susceptible to errors and misinterpretations compared to laboratory-based methods, LFAs are beneficial whenever the fields of application or resource-limited environments[203] require simplicity, low costs, short turnaround times, or self- and mass testing. In general, visually readable NP-based qualitative LFAs can provide sufficient clinical performance for the detection of analytes that are present in relatively high concentrations or when the change in analyte concentration is large enough to enable a simple binary readout, as in the case of pregnancy tests or testing of drugs of abuse in traffic controls.[3,204] The qualitative or, at best, semiquantitative results, however, limit the applicability of visually readable NP-based LFAs.[205] Many clinical applications and analytes require quantitative results, which is difficult to achieve based on a visual readout.

Compared to a visual detection, smartphone cameras enable a more sensitive, quantitative, and reproducible readout including color separation in RGB channels (**Figure 8**).[206,207] Smartphones are still compatible with PoC testing because they are already available even in resource-limited environments. Standardized and quantitative results require image processing by the smartphone to correct for image shape distortion, illumination brightness, and color imbalances.[208,209] Although even low-cost smartphones provide sufficient image processing power, new smartphone models only remain for a limited time on the market before being replaced by a new model. It is thus difficult for the LFA manufacturers to test them all. Thus, large-scale datasets consisting of real-world images are considered for the use in training and validation of image classification models. Furthermore, machine learning tools can be applied to optimize the readout and quantification of LFAs.[210,211]

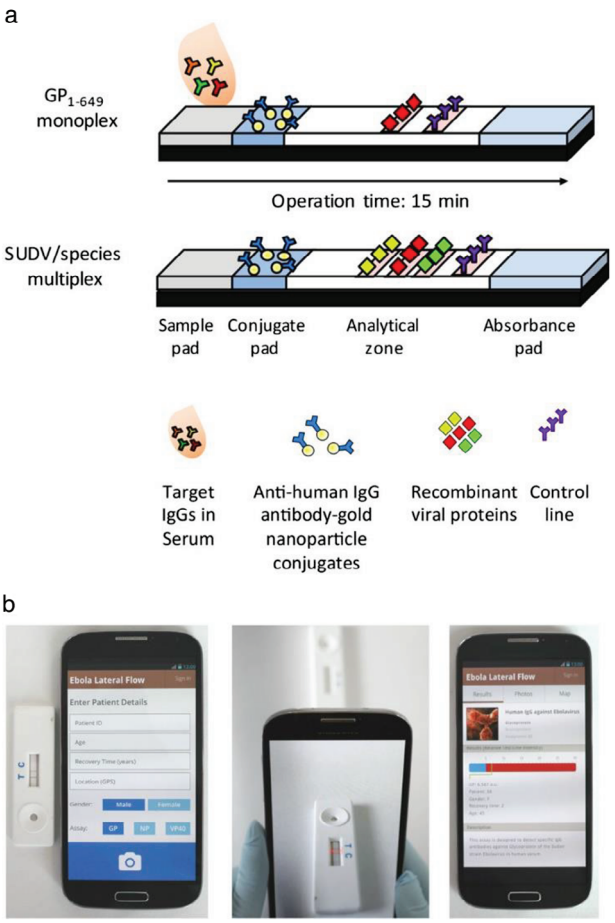


**Figure 8.** Smartphone-based LFA for the detection of antibodies against Ebola virus. a) After serum delivery, antibodies against viral proteins bind to test lines and the antihuman antibody–AuNP labels form a visual red-purple line. A control line confirms the assay function. b) A smartphone window shows the test results and patient details. When the red box is aligned between the test and control lines, their relative intensities indicate whether the result is positive or negative. Reproduced under the terms of the Creative Commons Attribution 4.0 International license.[206] Copyright 2018, the authors.

Some commercial test providers and public health agencies have already started to collect images for test registration and verification. This will enable not only reliable data analysis, but also continued improvements of image classification models. Furthermore, additional information can be linked to each measurement, enabling real-time, geo-linked surveillance.[210,212] For quantitative LFAs most commercial manufacturers develop and sell special detectors to correct the readout results.[213] The

integration of simple light-emitting diodes and photodiodes with readout electronics for colorimetric absorbance or reflectance measurements will ultimately enable the low-cost production of single-use LFA cartridges.[214]

Replacing the colorimetric labels by luminescent NPs can further strongly amplify the signal, which in principle should strongly increase the assay sensitivity.[215,216] LFAs, however, are a good example of an immunoassay platform, where the background fluorescence from the nitrocellulose material has impaired the detection of conventional fluorescence in practical applications.[217] Reducing the background fluorescence can thus improve the performance of LFAs more efficiently than increasing the label brightness. The time-gated luminescence from LnNPs[109] and the anti-Stokes luminescence from UCNPs have been employed in commercial LFAs for a sensitive luminescent detection without background fluorescence from nitrocellulose. UCNPs do not require a careful selection and optimization of the assay components or the optical components of the readout device for lower material background, which should result in lower expenses for both the test consumables and the readout instrument. Even minor differences in the manufacturing costs can provide a significant competitive advantage in the long run, especially, if the production scale is strongly increased over time. To estimate the total costs associated with a quantitative assay platform companies also need to take into account the development and manufacturing costs of the readout device.[218] Although the costs for the development of NP-based reagents are often higher, the overall assay costs per analyzed sample may actually be lower if the required readout devices are cheap and less complex.

The Chinese company Vazyme produces LFAs based on AuNPs for Covid-19 testing (antigen and antibodies) as well as QDs for a range of inflammatory and cardiovascular biomarkers. They also offer three fluorescence readout devices (QD-S600, QD-S900 and QD-S2000), which differ in sample throughput and the degree of assay automation.[219]

### 4.2. Mix-and-Measure (Homogeneous) Assays

The fluorescence polarization immunoassay—introduced in the 1960s—is probably the best-known homogeneous immunoassay that employs a (nano)size-dependent effect to measure immune complex formation. When polarized light excites a small fluorescent molecule in solution, the molecule rotates quickly between the time of excitation and emission, and thus the emission is unpolarized. After formation of an immune complex, however, the rotation slows down, and the fluorophore emits mainly light polarized in the same plane as the excitation source. Standard commercial applications do not require NPs, but as the depolarization depends on the size of the complex, a strong depolarization can in principle be achieved by using antibody–NP conjugates.

#### *4.2.1. Turbidimetric Immunoassays*

Turbidimetric immunoassays are a well-established scattering method widely used for the routine detection of clinical biomarkers in the laboratory.[220] The formation of immune complexes between the target analyte and the added antibody leads to an increase of the turbidity in the test sample, which can be measured with high throughput on automatic clinical chemistry analyzers. Traditional turbidimetric assays using free antibodies, however, are not sensitive enough for detecting low concentrations of biomarkers. Sub-micrometer particles (usually polystyrene) or NPs enhance the sensitivity based on a similar principle as common latex agglutination tests. Prominent examples are latex agglutination turbidimetric immunoassays and particle-enhanced turbidimetric immunoassays (PETIA). All major manufacturers produce such assays for a wide range of biomarkers.

The Norwegian company Gentian Diagnostics has commercialized PETIA assays utilizing antibody-coated polystyrene NPs. The open channel assays run on a wide range of automated clinical analyzers, which are already present in most clinical laboratories. Using existing infrastructure for the readout of new NP-based assays strongly increases the chance of a successful commercialization because there is no need for additional investment costs. Not all types of new assays, however, are compatible with existing laboratory equipment. The Finnish company Aidian has developed immunoturbidometric assays for PoC testing.

#### *4.2.2. Förster Resonance Energy Transfer (FRET)*

FRET assays typically consist of one antibody conjugated to a donor fluorophore and a second antibody conjugated to an acceptor fluorophore. If the analyte is bound by both antibodies, donor and acceptor come in close proximity. FRET between donor and acceptor results in a change of the fluorescence signal and may, e.g., switch on the acceptor emission. Though standard FRET pairs are based on fluorescent dyes, the detection scheme can be readily applied to NP-based donors and acceptors, in principle using various types of optical labels described in Section 3.3.

For example, upconversion resonance energy transfer was employed for the competitive detection of estradiol.[221] Donor UCNPs were modified with estradiol-specific antibodies and the acceptor dye Oyster-556 was conjugated to estradiol. In this competitive assay format, the sensitized acceptor lifetime emission was measured at 600 nm under continuous laser diode excitation at 980 nm. In general, however, there are not many commercial applications using FRET in combination with NPs, yet.

#### *4.2.3. Luminescence Oxygen Channeling*

The luminescence oxygen channeling immunoassay[30] is a commercially established homogeneous assay format that is only possible by using NPs. Two kinds of beads serve as the detection labels. First, beads coated with monoclonal antibodies and with incorporated chemiluminescent dye (chemibeads) are incubated with the sample, followed by the addition of biotinylated antibodies to form an immunocomplex with the target analyte. A second streptavidin-coated bead containing the photosensitizer (sensibead) is bound to the biotinylated antibody. Under 680 nm illumination, the sensibead generates singlet oxygen ($^1O_2$), which diffuses to the chemibead. The singlet oxygen triggers a chemiluminescent reaction in the chemibead, which is measured at 612 nm. Luminescence oxygen channeling immunoassays are available from Perkin Elmer (AlphaScreen) and Siemens Healthcare (Dimension Vista).[222]

## 5. Outlook on Commercialization Opportunities for New Assay Designs

At the end, we may break down our long discussion to a short question: "What is the difference between NP-based bioaffinity assays that are on the market and those that have not moved to the market?" If there was a given number of key parameters that assays must meet to be successful, their design would be straightforward. The first problem with this question, however, is that it is not a purely scientific one. Commercial success requires not only a competitive technology but also financial resources, business experience, and timely patent applications. The mindset and commitment of individuals to drive the technology toward market introduction—and to convince others on the way even if they cannot be sure that the product will eventually be successful—is essential. Overcoming all scientific, regulatory, and economic obstacles on the route to commercialization is typically associated with a large personal and financial risk.

Back in the scientific arena, a direct comparison of, e.g., the label brightness to fix the key parameters of bioaffinity assays is also not straightforward. In Section 3.3.2, we discussed that dye-doped NPs can strongly amplify the signal, but that this signal does not increase linearly with the number of fluorescent dyes due to quenching of the organic fluorophores. In LnNPs (Section 3.3.3), the overall brightness of each NP is more directly related to the number of enclosed Eu chelates. In an earlier quantitative experiment, Soukka et al.[223] compared the performance of an immunoassay using either individual Eu chelates as labels or EuNPs—each containing ≈30 000 Eu chelates—, which were about 4000× brighter than individual Eu chelate labeled antibodies. However, using otherwise exactly the same experimental conditions, the assay sensitivity improved only by a factor of 50 at best because the NPs led to a higher degree of nonspecific binding, which increased the background signal. In another study, AuNPs and EuNPs were compared as labels in an LFA for the detection of PSA.[106] The use of EuNPs improved the assay sensitivity but far below from what should be expected considering the highly improved detectability of EuNPs compared to AuNPs. This study clearly shows that it is not the NP brightness but rather the weak washing efficiency in LFAs, which leads to a relatively high background signal due to nonspecific binding and thus limits the assay sensitivity. These examples demonstrate that the signal amplification factors afforded by certain types of NPs do not turn directly into an improved assay sensitivity. In general, comparing individual assay parameters has a limited meaning for assessing the overall assay performance because the success of an assay depends on the entire concept of the platform technology.

Although bioaffinity assays using NPs as signal generating elements are already on the market, there are plenty of opportunities for the design of new assay concepts and platform technologies. The use of NPs as reagents and labels, however, poses additional challenges[224] for the development and validation of assays. In particular, a uniform and reproducible production and functionalization of NPs is necessary together with their stabilization for long-time storage in suspension to ensure that test kits yield highly reliable diagnostic results. The advantages conferred by the NPs in the assay performance must be strong enough compared to conventional molecular labels to justify the additional complexity and increased expenses associated with the development of NP-based products. Also, the management and mitigation of risks in the environment, health and safety need to be considered as there may be some (unknown) risks associated with the use of NP-based products.

The larger size of NPs compared to molecular labels may lead to steric hindrance in analyte recognition and slower the assay kinetics, which is an obvious disadvantage in bioaffinity assays. Steric restrictions of NPs may lead to problems in conventional microtiter plate or bead immunoassays[225] as well as in homogeneous immunoassays that rely on the specific binding interaction of two NPs.[226,227] The extent and likelihood of these steric issues depend on the NP size, coupling chemistry, the dimensions of the analyte, and how close to each other two epitopes are located on the analyte molecule targeted by the capture and detection antibodies.[133] Compared to molecular labels, NP-based assays require more optimization steps, which increase the amount of work and cost for the development of NP-based assays. Furthermore, the optimization work may be slowed down by the challenges associated with the characterization of the NP–antibody bioconjugates.[228,229] The binding reactivity of antibody-coated NP bioconjugates depends on the density of antibodies on the surface. A higher coating density and the proper orientation of antibodies improves their binding properties until a certain limit is reached.[14,230] Consequently, the consumption and costs of antibodies and reagents for the assay may increase when using larger NPs as a certain molar concentration of reactive NP bioconjugates is required in the assay—even if the total surface area per mass of NPs is decreased with larger NPs.

Certain optical features of NPs may enhance the assay performance beyond the options available for molecular optical labels and their conventional detectors. For example, it is not necessary to select and optimize the assay and optical components carefully regarding a lower background signal for the highly sensitive detection of UCNPs, which reduces the expenses for both the test consumables and the manufacturing of the readout instruments. These optical features may also be amenable for a readout by less sensitive but compact photodiode detectors[218] as compared to expensive and bulky photomultiplier tubes, which further reduces the overall price for the assay platform. Even minor differences in the manufacturing costs of consumables and readers can provide a significant competitive advantage in the long term, especially, if the production scale strongly increases with time.

While there are currently fewer NP-based labels found in commercial immunoassay platforms than one would expect from the large number of research articles, NP-based diagnostic PoC platforms have clearly shown their benefits and are already used in many commercial settings.[231] In the future, NP bioaffinity assays are foreseen to enable both affordable quantitative PoC testing and extremely sensitive tests with high technology level instrumentation.

## Acknowledgements

Z.F., P.S., and H.H.G. acknowledge funding from the Czech Science Foundation (GAČR GF23-06199K). [Correction added on 18 December 2023 after online publication: literatur references on page 6 and 11 are updated in this version.]

## Conflict of Interest

The authors declare no conflict of interest.

## Keywords

biosensor, Covid-19, digital assay, immunoassay, nanoparticle, point-of-care testing

Received: July 31, 2023
Revised: November 16, 2023
Published online:

[1] C. D. S. Brites, S. Balabhadra, L. D. Carlos, *Adv. Opt. Mater.* **2019**, *7*, 1801239.
[2] O. S. Wolfbeis, *Chem. Soc. Rev.* **2015**, *44*, 4743.
[3] A. Sena-Torralba, R. Álvarez-Diduk, C. Parolo, A. Piper, A. Merkoçi, *Chem. Rev.* **2022**, *122*, 14881.
[4] F. Hou, S. Sun, S. W. Abdullah, Y. Tang, X. Li, H. Guo, *Anal. Methods* **2023**, *15*, 2154.
[5] W. R. Algar, M. Massey, K. Rees, R. Higgins, K. D. Krause, G. H. Darwish, W. J. Peveler, Z. Xiao, H.-Y. Tsai, R. Gupta, K. Lix, M. V. Tran, H. Kim, *Chem. Rev.* **2021**, *121*, 9243.
[6] G. Kabay, J. Decastro, A. Altay, K. Smith, H.-W. Lu, A. M. Capossela, M. Moarefian, K. Aran, C. Dincer, *Adv. Mater.* **2022**, *34*, 2201085.
[7] J. L. Vaitukaitis, *Ann. N. Y. Acad. Sci.* **2004**, *1038*, 220.
[8] Lateral flow assays market, https://www.marketsandmarkets.com/Market-Reports/lateral-flow-assay-market-167205133.html (accessed: December 2023).
[9] C. D. Chin, V. Linder, S. K. Sia, *Lab Chip* **2012**, *12*, 2118.
[10] C. Selby, *Ann. Clin. Biochem.* **1999**, *36*, 704.
[11] D. R. Walt, *ACS Nano* **2009**, *3*, 2876.
[12] A. Frutiger, A. Tanno, S. Hwu, R. F. Tiefenauer, J. Vörös, N. Nakatsuka, *Chem. Rev.* **2021**, *121*, 8095.
[13] M. Mammen, S.-K. Choi, G. M. Whitesides, *Angew. Chem., Int. Ed.* **1998**, *37*, 2754.
[14] T. Soukka, H. Härmä, J. Paukkunen, T. Lövgren, *Anal. Chem.* **2001**, *73*, 2254.
[15] Z. Farka, M. J. Mickert, M. Pastucha, Z. Mikušová, P. Skládal, H. H. Gorris, *Angew. Chem., Int. Ed.* **2020**, *59*, 10746.
[16] A. Sedlmeier, H. H. Gorris, *Chem. Soc. Rev.* **2015**, *44*, 1526.
[17] A. Gnach, T. Lipinski, A. Bednarkiewicz, J. Rybka, J. A Capobianco, *Chem. Soc. Rev.* **2015**, *44*, 1561.
[18] S.-J. Kim, *Korean Circ. J.* **2021**, *51*, 997.
[19] C. S. Wood, M. R. Thomas, J. Budd, T. P. Mashamba-Thompson, K. Herbst, D. Pillay, R. W. Peeling, A. M. Johnson, R. A. Mckendry, M. M. Stevens, *Nature* **2019**, *566*, 467.
[20] H. Kim, D.-R. Chung, M. Kang, *Analyst* **2019**, *144*, 2460.
[21] H. van Poppel, R. Hogenhout, P. Albers, R. C. N. van den Bergh, J. O. Barentsz, M. J. Roobol, *Eur. Urol.* **2021**, *79*, 327.
[22] A. Maj-Hes, S. Sevcenco, T. Szarvas, G. Kramer, *Adv. Ther.* **2019**, *36*, 916.
[23] R. S. Niedbala, H. Feindt, K. Kardos, T. Vail, J. Burton, B. Bielska, S. Li, D. Milunic, P. Bourdelle, R. Vallejo, *Anal. Biochem.* **2001**, *293*, 22.
[24] T. Aubert, A. A. Golovatenko, M. Samoli, L. Lermusiaux, T. Zinn, B. Abécassis, A. V. Rodina, Z. Hens, *Nano Lett.* **2022**, *22*, 1778.
[25] X. Fan, W. Zheng, D. J. Singh, *Light: Sci. Appl.* **2014**, *3*, e179.
[26] N. A. Byzova, A. V. Zherdev, B. N. Khlebtsov, A. M. Burov, N. G. Khlebtsov, B. B. Dzantiev, *Sensors* **2020**, *20*, 3608.
[27] S. Dühnen, T. Rinkel, M. Haase, *Chem. Mater.* **2015**, *27*, 4033.
[28] H. de Puig, I. Bosch, M. Carré-Camps, K. Hamad-Schifferli, *Bioconjugate Chem.* **2017**, *28*, 230.
[29] R. Rampado, S. Crotti, P. Caliceti, S. Pucciarelli, M. Agostini, *Front. Bioeng. Biotechnol.* **2020**, *8*, 166.
[30] E. F. Ullman, H. Kirakossian, S. Singh, Z. P. Wu, B. R. Irvin, J. S. Pease, A. C. Switchenko, J. D. Irvine, A. Dafforn, C. N. Skold, *Proc. Natl. Acad. Sci. USA* **1994**, *91*, 5426.
[31] D. Lou, L. Fan, T. Jiang, Y. Zhang, *VIEW* **2022**, *3*, 20200125.
[32] S. M. Talha, T. Salminen, E. Juntunen, A. Spangar, C. Gurramkonda, T. Vuorinen, N. Khanna, K. Pettersson, *J. Virol. Methods* **2016**, *229*, 66.
[33] A. Hlaváček, M. Peterek, Z. Farka, M. J. Mickert, L. Prechtl, D. Knopp, H. H. Gorris, *Microchim. Acta* **2017**, *184*, 4159.
[34] H. Péré, I. Podglajen, M. Wack, E. Flamarion, T. Mirault, G. Goudot, C. Hauw-Berlemont, L. Le, E. Caudron, S. Carrabin, J. Rodary, T. Ribeyre, L. Bélec, D. Veyer, *J. Clin. Microbiol.* **2020**, *58*, 2.
[35] S. Madhu, A. J. Anthuuvan, S. Ramasamy, P. Manickam, S. Bhansali, P. Nagamony, V. Chinnuswamy, *ACS Appl. Electron. Mater.* **2020**, *2*, 499.
[36] M. Pastucha, Z. Farka, K. Lacina, Z. Mikusová, P. Skládal, *Microchim. Acta* **2019**, *186*, 312.
[37] R. Peltomaa, R. Barderas, E. Benito-Peña, M. C. Moreno-Bondi, *Anal. Bioanal. Chem.* **2022**, *414*, 193.
[38] B. T. S. Bui, K. Haupt, *Anal. Bioanal. Chem.* **2010**, *398*, 2481.
[39] S. M. Biros, J. Rebek Jr., *Chem. Soc. Rev.* **2007**, *36*, 93.
[40] S. Waxman, C. Schreiber, *Blood* **1973**, *42*, 281.
[41] K. Gidwani, K. Huhtinen, H. Kekki, S. van Vliet, J. Hynninen, N. Koivuviita, A. Perheentupa, M. Poutanen, A. Auranen, S. Grenman, U. Lamminmäki, O. Carpen, Y. van Kooyk, K. Pettersson, *Clin. Chem.* **2016**, *62*, 1390.
[42] J. Foote, H. N. Eisen, *Proc. Natl. Acad. Sci. USA* **1995**, *92*, 1254.
[43] P. J. Conroy, S. Hearty, P. Leonard, R. J. O'kennedy, *Semin. Cell Dev. Biol.* **2009**, *20*, 10.
[44] S. Sharma, H. Byrne, R. J. O'Kennedy, *Essays Biochem.* **2016**, *60*, 9.
[45] Z. Farka, T. S. Juřík, D. Kovář, L. Trnková, P. Skládal, *Chem. Rev.* **2017**, *117*, 9973.
[46] G. Köhler, C. Milstein, *Nature* **1975**, *256*, 495.
[47] H.-J. Jeong, T. Kawamura, J. Dong, H. Ueda, *ACS Sens.* **2016**, *1*, 88.
[48] C. Hamers-Casterman, T. Atarhouch, S. Muyldermans, G. Robinson, C. Hammers, E. B. Songa, N. Bendahman, R. Hammers, *Nature* **1993**, *363*, 446.
[49] K. Juarez, G. Dubberke, P. Lugo, F. Koch-Nolte, F. Buck, F. Haag, A. Licea, *Hybridoma* **2011**, *30*, 323.
[50] M. J. Feige, M. A. Gräwert, M. Marcinowski, J. Hennig, J. Behnke, D. Ausländer, E. M. Herold, J. Peschek, C. D. Castro, M. Flajnik, L. M. Hendershot, M. Sattler, M. Groll, J. Buchner, *Proc. Natl. Acad. Sci USA* **2014**, *111*, 8155.
[51] J.-P. Salvador, L. Vilaplana, M.-P. Marco, *Anal. Bioanal. Chem.* **2019**, *411*, 1703.
[52] M. Liu, L. Li, D. Jin, Y. Liu, *Wiley Interdisp. Rev. Nanomed. Nanobiotechnol.* **2021**, *13*, 1697.
[53] G. Hassanzadeh-Ghassabeh, N. Devoogdt, P. de Pauw, C. Vincke, S. Muyldermans, *Nanomedicine* **2013**, *8*, 1013.
[54] R. Su, Y.-T. Wu, S. Doulkeridou, X. Qiu, T. J. Sørensen, K. Susumu, I. L. Medintz, P. M. P. van Bergen en Henegouwen, N. Hildebrandt, *Angew. Chem., Int. Ed.* **2022**, *61*, 202207797.
[55] A. Conidi, V. van den Berghe, D. Huylebroeck, *Int. J. Mol. Sci.* **2013**, *14*, 6690.
[56] F. Li, Z. Yu, X. Han, R. Y. Lai, *Anal. Chim. Acta* **2019**, *1051*, 1.
[57] R. Stoltenburg, C. Reinemann, B. Strehlitz, *Biomol. Eng.* **2007**, *24*, 381.
[58] M. Mascini, I. Palchetti, S. Tombelli, *Angew. Chem., Int. Ed.* **2012**, *51*, 1316.

[59] L. S. Rotherham, C. Maserumule, K. Dheda, J. Theron, M. Khati, *PLoS One* **2012**, *7*, 46862.
[60] A. Kinghorn, L. Fraser, S. Liang, S. Shiu, J. Tanner, *Int. J. Mol. Sci.* **2017**, *18*, 2516.
[61] S. M. Shaban, D.-H. Kim, *Sensors* **2021**, *21*, 979.
[62] S. Y. Toh, M. Citartan, S. C. B. Gopinath, T.-H. Tang, *Biosens. Bioelectron.* **2015**, *64*, 392.
[63] Z.-S. Wu, M.-M. Guo, S.-B. Zhang, Chen, J.-H. Jiang, G.-L. Shen, R.-Q. Yu, *Anal. Chem.* **2007**, *79*, 2933.
[64] V. Thiviyanathan, D. G. Gorenstein, *Proteomics: Clin. Appl.* **2012**, *6*, 563.
[65] B. Strehlitz, C. Reinemann, S. Linkorn, R. Stoltenburg, *Bioanal. Rev.* **2012**, *4*, 1.
[66] M. Berezovski, M. Musheev, A. Drabovich, S. N. Krylov, *J. Am. Chem. Soc.* **2006**, *128*, 1410.
[67] S. Reverdatto, D. Burz, A. Shekhtman, *Curr. Top. Med. Chem.* **2015**, *15*, 1082.
[68] R. R. Tonelli, W. Colli, M. J. M. Alves, *Front. Immunol.* **2013**, *3*, 419.
[69] A. Yarman, S. Kurbanoglu, I. Zebger, F. W. Scheller, *Sens. Actuators, B* **2021**, *330*, 129369.
[70] K. Haupt, K. Mosbach, *Chem. Rev.* **2000**, *100*, 2495.
[71] O. S. Ahmad, T. S. Bedwell, C. Esen, A. Garcia-Cruz, S. A. Piletsky, *Trends Biotechnol.* **2019**, *37*, 294.
[72] A. A. Hasseb, N. D. T. Abdel Ghani, O. R. Shehab, R. M. El Nashar, *Curr. Opin. Electrochem.* **2022**, *31*, 100848.
[73] T. S. Bedwell, M. J. Whitcombe, *Anal. Bioanal. Chem.* **2016**, *408*, 1735.
[74] N. Tarannum, O. D. Hendrickson, S. Khatoon, A. V. Zherdev, B. B. Dzantiev, *Crit. Rev. Anal. Chem.* **2020**, *50*, 291.
[75] G. Becskereki, G. Horvai, B. Tóth, *Polymers* **2021**, *13*, 1781.
[76] J. Mcclements, L. Bar, P. Singla, F. Canfarotta, A. Thomson, J. Czulak, R. E. Johnson, R. D. Crapnell, C. E. Banks, B. Payne, S. Seyedin, P. Losada-Pérez, M. Peeters, *ACS Sens.* **2022**, *7*, 1122.
[77] H. Altug, S.-H. Oh, S. A. Maier, J. Homola, *Nat. Nanotechnol.* **2022**, *17*, 5.
[78] N. Wongkaew, M. Simsek, C. Griesche, A. J. Baeumner, *Chem. Rev.* **2019**, *119*, 120.
[79] S. J. Osterfeld, S. X. Wang, in *Microarrays: Preparation, Microfluidics, Detection Methods, and Biological Applications* (Eds: K. Dill, R. H. Liu, P. Grodzinski), Springer, New York, NY **2009**, pp. 299–314.
[80] N. N. Trivedi, J. K Brown, T. Rubenstein, A. D Rostykus, A. L Fish, H. Yu, L. Carbonell, A. Juang, S. Kamer, B. Patel, M. Sidhu, D. Vuong, S. Wang, M. Beggs, A. Hb Wu, M. Arjomandi, *Biomed. Res. Rev.* **2018**, *2*, 1.
[81] C. Fenzl, T. Hirsch, A. J. Baeumner, *TrAC, Trends Anal. Chem.* **2016**, *79*, 306.
[82] L. Zhang, Y. Mazouzi, M. Salmain, B. Liedberg, S. Boujday, *Biosens. Bioelectron.* **2020**, *165*, 112370.
[83] C. J. Murphy, A. M. Gole, J. W. Stone, P. N. Sisco, A. M. Alkilany, E. C. Goldsmith, S. C. Baxter, *Acc. Chem. Res.* **2008**, *41*, 1721.
[84] A. J. Haes, R. P. van Duyne, *Anal. Bioanal. Chem.* **2004**, *379*, 920.
[85] J. Turkevich, P. C. Stevenson, J. Hillier, *Discuss. Faraday Soc.* **1951**, *11*, 55.
[86] G. Frens, *Nat. Phys. Sci.* **1973**, *241*, 20.
[87] Y. Xia, Y. Xiong, B. Lim, S. E. Skrabalak, *Angew. Chem., Int. Ed.* **2009**, *48*, 60.
[88] R. Liu, Y. Zhang, S. Zhang, W. Qiu, Y. Gao, *Appl. Spectrosc. Rev.* **2014**, *49*, 121.
[89] X. Wang, R. Niessner, D. Tang, D. Knopp, *Anal. Chim. Acta* **2016**, *912*, 10.
[90] H.-Y. Lin, C.-H. Huang, S.-H. Lu, I.-T. Kuo, L.-K. Chau, *Biosens. Bioelectron.* **2014**, *51*, 371.
[91] F. Inci, C. Filippini, M. Baday, M. O. Ozen, S. Calamak, N. G. Durmus, S. Wang, E. Hanhauser, K. S. Hobbs, F. Juillard, P. P. Kuang, M. L. Vetter, M. Carocci, H. S. Yamamoto, Y. Takagi, U. H. Yildiz, D. Akin, D. R. Wesemann, A. Singhal, P. L. Yang, M. L. Nibert, R. N. Fichorova, D. T.-Y. Lau, T. J. Henrich, K. M. Kaye, S. C. Schachter, D. R. Kuritzkes, L. M. Steinmetz, S. S. Gambhir, R. W. Davis, et al., *Proc. Natl. Acad. Sci. USA* **2015**, *112*, 4354.
[92] C.-C. Chang, C.-P. Chen, T.-H. Wu, C.-H. Yang, C.-W. Lin, C.-Y. Chen, *Nanomaterials* **2019**, *9*, 861.
[93] H. Jans, Q. Huo, *Chem. Soc. Rev.* **2012**, *41*, 2849.
[94] L. Khelifa, Y. Hu, N. Jiang, A. K. Yetisen, *Lab Chip* **2022**, *22*, 2451.
[95] S. Mayilo, M. A. Kloster, M. Wunderlich, A. Lutich, T. A. Klar, A. Nichtl, K. Kürzinger, F. D. Stefani, J. Feldmann, *Nano Lett.* **2009**, *9*, 4558.
[96] J. Wan, J. Ai, Y. Zhang, X. Geng, Q. Gao, Z. Cheng, *Sci. Rep.* **2016**, *6*, 19806.
[97] M.-Q. He, Y.-L. Yu, J.-H. Wang, *Nano Today* **2020**, *35*, 101005.
[98] P. Zhao, Y. Chen, Y. Chen, S. Hu, H. Chen, W. Xiao, G. Liu, Y. Tang, J. Shi, Z. He, Y. Luo, Z. Chen, *J. Mater. Chem. C* **2020**, *8*, 6861.
[99] U. S. Dinish, G. Balasundaram, Y.-T. Chang, M. Olivo, *Sci. Rep.* **2014**, *4*, 4075.
[100] M. Montalti, L. Prodi, E. Rampazzo, N. Zaccheroni, *Chem. Soc. Rev.* **2014**, *43*, 4243.
[101] A. Reisch, P. Didier, L. Richert, S. Oncul, Y. Arntz, Y. Mély, A. S. Klymchenko, *Nat. Commun.* **2014**, *5*, 4089.
[102] C. Hofmann, A. Duerkop, A. J. Baeumner, *Angew. Chem., Int Ed.* **2019**, *58*, 12840.
[103] X.-D. Wang, H. H. Gorris, J. A. Stolwijk, R. J. Meier, D. B. M. Groegel, J. Wegener, O. S. Wolfbeis, *Chem. Sci.* **2011**, *2*, 901.
[104] S. M. Borisov, T. Mayr, G. Mistlberger, I. Klimant, in *Advanced Fluorescence Reporters in Chemistry and Biology II: Molecular Constructions, Polymers and Nanoparticles* (Ed: A. P. Demchenko), Springer, Berlin **2010**, pp. 193–228.
[105] T. I. Koshy, K. F. Buechler, in *The Immunoassay Handbook* (Ed: D. Wild), 4th ed., Elsevier, Oxford, UK **2013**, pp. 541–544.
[106] E. Juntunen, T. Myyryläinen, T. Salminen, T. Soukka, K. Pettersson, *Anal. Biochem.* **2012**, *428*, 31.
[107] H. Härmä, T. Soukka, T. Lövgren, *Clin. Chem.* **2001**, *47*, 561.
[108] X. Xia, Y. Xu, X. Zhao, Q. Li, *Clin. Chem.* **2009**, *55*, 179.
[109] G. Rundström, A. Jonsson, O. Mårtensson, I. Mendel-Hartvig, P. Venge, *Clin. Chem.* **2007**, *53*, 342.
[110] L. Kokko, T. Lövgren, T. Soukka, *Anal. Chim. Acta* **2007**, *585*, 17.
[111] Y. Zhang, F. Ren, G. Wang, T. Liao, Y. Hao, H. Zhang, *Sens. Actuators, B* **2021**, *329*, 129273.
[112] F. Mousseau, C. Féraudet Tarisse, S. Simon, T. Gacoin, A. Alexandrou, C. I. Bouzigues, *Nanoscale* **2021**, *13*, 14814.
[113] J. Y. Ham, J. Jung, B.-G. Hwang, W.-J. Kim, Y.-S. Kim, E.-J. Kim, M.-Y. Cho, M.-S. Hwang, D. I. Won, J. S. Suh, *Ann. Lab. Med.* **2015**, *35*, 50.
[114] D. Bera, L. Qian, T.-K. Tseng, P. H. Holloway, *Materials* **2010**, *3*, 2260.
[115] A. M. Smith, S. Nie, *Acc. Chem. Res.* **2010**, *43*, 190.
[116] N. Hildebrandt, C. M. Spillmann, W. R. Algar, T. Pons, M. H. Stewart, E. Oh, K. Susumu, S. A. Díaz, J. B. Delehanty, I. L. Medintz, *Chem. Rev.* **2017**, *117*, 536.
[117] A. Fu, W. Gu, C. Larabell, A. P. Alivisatos, *Curr. Opin. Neurobiol.* **2005**, *15*, 568.
[118] E. Petryayeva, W. R. Algar, I. L. Medintz, *Appl. Spectrosc.* **2013**, *67*, 215.
[119] U. Resch-Genger, M. Grabolle, S. Cavaliere-Jaricot, R. Nitschke, T. Nann, *Nat. Methods* **2008**, *5*, 763.
[120] B. Ballou, B. C. Lagerholm, L. A. Ernst, M. P. Bruchez, A. S. Waggoner, *Bioconjugate Chem.* **2004**, *15*, 79.
[121] W. R. Algar, A. J. Tavares, U. J. Krull, *Anal. Chim. Acta* **2010**, *673*, 1.
[122] Z. A. Peng, X. Peng, *J. Am. Chem. Soc.* **2001**, *123*, 183.
[123] I. L. Medintz, H. T. Uyeda, E. R. Goldman, H. Mattoussi, *Nat. Mater.* **2005**, *4*, 435.

[124] W. W. Yu, E. Chang, R. Drezek, V. L. Colvin, *Biochem. Biophys. Res. Commun.* **2006**, *348*, 781.
[125] E. E. Lees, T.-L. Nguyen, A. H. A. Clayton, P. Mulvaney, *ACS Nano* **2009**, *3*, 1121.
[126] M. Díaz-González, A. de la Escosura-Muñiz, M. T. Fernandez-Argüelles, F. J. G. Alonso, J. M. Costa-Fernandez, in *Surface-modified Nanobiomaterials for Electrochemical and Biomedicine Applications* (Eds: A. R. Puente-Santiago, D. Rodríguez-Padrón), Springer International Publishing, Cham **2020**, pp. 133–176.
[127] B. Fang, Q. Xiong, H. Duan, Y. Xiong, W. Lai, *TrAC, Trends Anal. Chem.* **2022**, *157*, 116754.
[128] M. Cardoso Dos Santos, W. R. Algar, I. L. Medintz, N. Hildebrandt, *TrAC, Trends Anal. Chem.* **2020**, *125*, 115819.
[129] E. Yang, Y. Zhang, Y. Shen, *Anal. Chim. Acta* **2022**, *1209*, 339140.
[130] P. Wu, X.-P. Yan, *Chem. Soc. Rev.* **2013**, *42*, 5489.
[131] S. Kargozar, S. J. Hoseini, P. B. Milan, S. Hooshmand, H.-W. Kim, M. Mozafari, *Biotechnol. J.* **2020**, *15*, 2000117.
[132] M. Han, X. Gao, J. Z. Su, S. Nie, *Nat. Biotechnol.* **2001**, *19*, 631.
[133] A.-C. Mirica, D. Stan, I.-C. Chelcea, C. M. Mihailescu, A. Ofiteru, L.-A. Bocancia-Mateescu, *Front. Bioeng. Biotechnol.* **2022**, *10*, 922772.
[134] S.-K. Kim, H. Sung, S.-H. Hwang, M.-N. Kim, *BioChip J.* **2022**, *16*, 175.
[135] L. Feng, C. Zhu, H. Yuan, L. Liu, F. Lv, S. Wang, *Chem. Soc. Rev.* **2013**, *42*, 6620.
[136] Y. Wang, L. Feng, S. Wang, *Adv. Funct. Mater.* **2019**, *29*, 1806818.
[137] S. Sarkar, N. Levi-Polyachenko, *Adv. Drug Delivery Rev.* **2020**, *163–164*, 40.
[138] C. Zhu, L. Liu, Q. Yang, F. Lv, S. Wang, *Chem. Rev.* **2012**, *112*, 4687.
[139] J. Yu, Y. Rong, C.-T. Kuo, X.-H. Zhou, D. T. Chiu, *Anal. Chem.* **2017**, *89*, 42.
[140] P.-Y. You, F.-C. Li, M.-H. Liu, Y.-H. Chan, *ACS Appl. Mater. Interfaces* **2019**, *11*, 9841.
[141] Y.-Q. Yang, Y.-C. Yang, M.-H. Liu, Y.-H. Chan, *Anal. Chem.* **2020**, *92*, 1493.
[142] Y.-C. Yang, M.-H. Liu, S.-M. Yang, Y.-H. Chan, *ACS Sens.* **2021**, *6*, 4255.
[143] M. Haase, H. Schäfer, *Angew. Chem., Int. Ed.* **2011**, *50*, 5808.
[144] X. Li, F. Zhang, D. Zhao, *Chem. Soc. Rev.* **2015**, *44*, 1346.
[145] C. Homann, L. Krukewitt, F. Frenzel, B. Grauel, C. Würth, U. Resch-Genger, M. Haase, *Angew. Chem., Int. Ed.* **2018**, *57*, 8765.
[146] A. Hlaváček, Z. Farka, M. J. Mickert, U. Kostiv, J. C. Brandmeier, D. Horák, P. Skládal, F. Foret, H. H. Gorris, *Nat. Protoc.* **2022**, *17*, 1028.
[147] A. L. Ouellette, J. J. Li, D. E. Cooper, A. J. Ricco, G. T. A. Kovacs, *Anal. Chem.* **2009**, *81*, 3216.
[148] K. Raiko, A. Lyytikäinen, M. Ekman, A. Nokelainen, S. Lahtinen, T. Soukka, *Clin. Chim. Acta* **2021**, *523*, 380.
[149] H. J. Tanke, M. Zuiderwijk, K. Wiesmeijer, R. Breedveld, W. Abrams, C. J. de Dood, E. Tjon Kon Fat, P. L. A. Corstjens, *Proc. SPIE* **2014**, *8947*.
[150] P. L. A. M. Corstjens, C. J. de Dood, J. W. Priest, H. J. Tanke, S. Handali, *PLoS Neglected Trop. Dis.* **2014**, *8*, 2944.
[151] H. H. Gorris, R. Ali, S. M. Saleh, O. S. Wolfbeis, *Adv. Mater.* **2011**, *23*, 1652.
[152] J. C. Brandmeier, K. Raiko, Z. Farka, R. Peltomaa, M. J. Mickert, A. Hlaváček, P. Skládal, T. Soukka, H. H. Gorris, *Adv. Healthcare Mater.* **2021**, *10*, 2100506.
[153] H. He, B. Liu, S. Wen, J. Liao, G. Lin, J. Zhou, D. Jin, *Anal. Chem.* **2018**, *90*, 12356.
[154] A. Sedlmeier, A. Hlaváček, L. Birner, M. J. Mickert, V. Muhr, T. Hirsch, P. L. A. M. Corstjens, H. J. Tanke, T. Soukka, H. H. Gorris, *Anal. Chem.* **2016**, *88*, 1835.
[155] S. Bayoumy, H. Hyytiä, J. Leivo, S. M. Talha, K. Huhtinen, M. Poutanen, J. Hynninen, A. Perheentupa, U. Lamminmäki, K. Gidwani, K. Pettersson, *Commun. Biol.* **2020**, *3*, 460.
[156] I. Martiskainen, S. M. Talha, K. Vuorenpää, T. Salminen, E. Juntunen, S. Chattopadhyay, D. Kumar, T. Vuorinen, K. Pettersson, N. Khanna, G. Batra, *Anal. Bioanal. Chem.* **2021**, *413*, 967.
[157] H. Li, W. Ahmad, Y. Rong, Q. Chen, M. Zuo, Q. Ouyang, Z. Guo, *Food Control* **2020**, *107*, 106761.
[158] E. Makhneva, D. Sklenárová, J. C. Brandmeier, A. Hlaváček, H. H. Gorris, P. Skládal, Z. Farka, *Anal. Chem.* **2022**, *94*, 16376.
[159] Z. Farka, M. J. Mickert, Z. Mikusová, A. Hlaváček, P. Bouchalová, W. Xu, P. Bouchal, P. Skládal, H. H. Gorris, *Nanoscale* **2020**, *12*, 8303.
[160] F. van de Rijke, H. Zijlmans, S. Li, T. Vail, A. K. Raap, R. S. Niedbala, H. J. Tanke, *Nat. Biotechnol.* **2001**, *19*, 273.
[161] T. Lidström, J. Cumming, R. Gaur, L. Frängsmyr, I. S. Pateras, M. J. Mickert, O. Franklin, M. N. E. Forsell, N. Arnberg, M. Dongre, C. Patthey, D. Öhlund, *Cancer Immunol. Res.* **2023**, *11*, 72.
[162] D. L. Rimm, *Nat. Biotechnol.* **2006**, *24*, 914.
[163] S.-K. Sun, H.-F. Wang, X.-P. Yan, *Acc. Chem. Res.* **2018**, *51*, 1131.
[164] S. Wu, Y. Li, W. Ding, L. Xu, Y. Ma, L. Zhang, *Nano-Micro Lett.* **2020**, *12*, 70.
[165] N. Liu, X. Chen, X. Sun, X. Sun, J. Shi, *J. Nanobiotechnol.* **2021**, *19*, 113.
[166] B.-Y. Wu, H.-F. Wang, J.-T. Chen, X.-P. Yan, *J. Am. Chem. Soc.* **2011**, *133*, 686.
[167] A. S. Paterson, B. Raja, G. Garvey, A. Kolhatkar, A. E. V. Hagström, K. Kourentzi, T. R. Lee, R. C. Willson, *Anal. Chem.* **2014**, *86*, 9481.
[168] Y. Wang, B. Yan, L. Chen, *Chem. Rev.* **2013**, *113*, 1391.
[169] X. Zhao, M. Li, Z. Xu, *Front. Microbiol.* **2018**, *9*, 1236.
[170] S. Cheng, Z. Tu, S. Zheng, X. Cheng, H. Han, C. Wang, R. Xiao, B. Gu, *Anal. Chim. Acta* **2021**, *1187*, 339155.
[171] H. Liu, E. Dai, R. Xiao, Z. Zhou, M. Zhang, Z. Bai, Y. Shao, K. Qi, J. Tu, C. Wang, S. Wang, *Sens. Actuators, B* **2021**, *329*, 129196.
[172] I. V. Safenkova, V. G. Panferov, N. A. Panferova, Y. A. Varitsev, A. V. Zherdev, B. B. Dzantiev, *Talanta* **2019**, *195*, 739.
[173] Y. Huang, H. Zhu, *Genomics, Proteomics Bioinf.* **2017**, *15*, 73.
[174] S. Fournier-Bidoz, T. L. Jennings, J. M. Klostranec, W. Fung, A. Rhee, D. Li, W. C. W. Chan, *Angew. Chem., Int. Ed.* **2008**, *47*, 5577.
[175] E. R. Goldman, A. R. Clapp, G. P. Anderson, H. T. Uyeda, J. M. Mauro, I. L. Medintz, H. Mattoussi, *Anal. Chem.* **2004**, *76*, 684.
[176] C. N. Lafratta, D. R. Walt, *Chem. Rev.* **2008**, *108*, 614.
[177] Y. Lu, J. Zhao, R. Zhang, Y. Liu, D. Liu, E. M. Goldys, X. Yang, P. Xi, A. Sunna, J. Lu, Y. Shi, R. C. Leif, Y. Huo, J. Shen, J. A. Piper, J. P. Robinson, D. Jin, *Nat. Photonics* **2014**, *8*, 32.
[178] S. A. Dunbar, *Clin. Chim. Acta* **2006**, *363*, 71.
[179] P. Carl, D. Sarma, B. J. R. Gregório, K. Hoffmann, A. Lehmann, K. Rurack, R. J. Schneider, *Anal. Chem.* **2019**, *91*, 12988.
[180] H. Liu, Y. Lei, *Biosens. Bioelectron.* **2021**, *177*, 112901.
[181] D. M. Rissin, C. W. Kan, T. G. Campbell, S. C. Howes, D. R. Fournier, L. Song, T. Piech, P. P. Patel, L. Chang, A. J. Rivnak, E. P. Ferrell, J. D. Randall, G. K. Provuncher, D. R. Walt, D. C. Duffy, *Nat. Biotechnol.* **2010**, *28*, 595.
[182] D. M. Rissin, D. R. Walt, *Nano Lett.* **2006**, *6*, 520.
[183] M. J. Mickert, Z. Farka, U. Kostiv, A. Hlaváček, D. Horák, P. Skládal, H. H. Gorris, *Anal. Chem.* **2019**, *91*, 9435.
[184] Z. Farka, M. J. Mickert, A. Hlaváček, P. Skládal, H. H. Gorris, *Anal. Chem.* **2017**, *89*, 11825.
[185] J. C. Brandmeier, N. Jurga, T. Grzyb, A. Hlaváček, R. Oborilová, P. Skládal, Z. Farka, H. H. Gorris, *Anal. Chem.* **2023**, *95*, 4753.
[186] M. Sriram, B. P. Markhali, P. R. Nicovich, D. T. Bennett, P. J. Reece, D. Brynn Hibbert, R. D. Tilley, K. Gaus, S. R. C. Vivekchand, J. J. Gooding, P. J. Reece, D., B. H., R. D. Tilley, K. Gaus, S. R. C. Vivekchand, J. J. Gooding, *Biosens. Bioelectron.* **2018**, *117*, 530.

[187] Y. Liu, H. Ye, H. Huynh, C. Xie, P. Kang, J. S. Kahn, Z. Qin, *Nat. Commun.* **2022**, *13*, 1687.
[188] L. Mou, X. Jiang, *Adv. Healthcare Mater.* **2017**, *6*, 1601403.
[189] D. Wild, *The Immunoassay Handbook*, 4th ed., Elsevier, New York **2013**.
[190] H. H. Gorris, T. Soukka, *Anal. Chem.* **2022**, *94*, 6073.
[191] K. Mosbach, L. Andersson, *Nature* **1977**, *270*, 259.
[192] D. M. Bruls, T. H. Evers, J. A. H. Kahlman, P. J. W. van Lankvelt, M. Ovsyanko, E. G. M. Pelssers, J. J. H. B. Schleipen, F. K. de Theije, C. A. Verschuren, T. van der Wijk, J. B. A. van Zon, W. U. Dittmer, A. H. J. Immink, J. H. Nieuwenhuis, M. W. J. Prins, *Lab Chip* **2009**, *9*, 3504.
[193] B. O'Farrell, in *Lateral Flow Immunoassay* (Ed: R. Wong, H. Tse), Humana Press, Totowa, NJ **2009**, pp. 1–33.
[194] Q. H. Nguyen, M. I. Kim, *TrAC, Trends Anal. Chem.* **2020**, *132*, 116038.
[195] D. Quesada-González, A. Merkoçi, *Biosens. Bioelectron.* **2015**, *73*, 47.
[196] *Lateral flow Assay Market Size and Forecast*, https://www.verifiedmarketresearch.com/product/lateral-flow-assay-market (accessed: December 2023).
[197] Z. F. Igloi, J. Velzing, J. van Beek, D. van de Vijver, G. Aron, R. Ensing, K. Benschop, W. Han, T. Boelsums, M. Koopmans, C. Geurtsvankessel, R. Molenkamp, *Emerging Infect. Dis.* **2021**, *27*, 1323.
[198] F. di Nardo, M. Chiarello, S. Cavalera, C. Baggiani, L. Anfossi, *Sensors* **2021**, *21*, 5185.
[199] Y. Zhou, Y. Wu, L. Ding, X. Huang, Y. Xiong, *TrAC, Trends Anal. Chem.* **2021**, *145*, 116452.
[200] H. R. Boehringer, B. J. O'farrell, *Clin. Chem.* **2021**, *68*, 52.
[201] M. J. Loeffelholz, Y.-W. Tang, *Bioanalysis* **2021**, *13*, 1213.
[202] G. Guglielmi, *Nature* **2021**, *590*, 202.
[203] K. Ratajczak, M. Stobiecka, *Carbohydr. Polym.* **2020**, *229*, 115463.
[204] O. Miocevic, C. R. Cole, M. J. Laughlin, R. L. Buck, P. D. Slowey, E. A. Shirtcliff, *Front. Public Health* **2017**, *5*, 133.
[205] Z. Wang, J. Zhao, X. Xu, L. Guo, L. Xu, M. Sun, S. Hu, H. Kuang, C. Xu, A. Li, *Small Methods* **2022**, *6*, 2101143.
[206] P. Brangel, A. Sobarzo, C. Parolo, B. S. Miller, P. D. Howes, S. Gelkop, J. J. Lutwama, J. M. Dye, R. A. Mckendry, L. Lobel, M. M. Stevens, *ACS Nano* **2018**, *12*, 63.
[207] C. Ruppert, N. Phogat, S. Laufer, M. Kohl, H.-P. Deigner, *Microchim. Acta* **2019**, *186*, 119.
[208] A. K. Yetisen, M. S. Akram, C. R. Lowe, *Lab Chip* **2013**, *13*, 2210.
[209] J.-H. Park, E.-K. Park, Y. K. Cho, I.-S. Shin, H. Lee, *ACS Omega* **2022**, *7*, 17723.
[210] J. Budd, B. S. Miller, N. E. Weckman, D. Cherkaoui, D. Huang, A. T. Decruz, N. Fongwen, G.-R. Han, M. Broto, C. S. Estcourt, J. Gibbs, D. Pillay, P. Sonnenberg, R. Meurant, M. R. Thomas, N. Keegan, M. M. Stevens, E. Nastouli, E. J. Topol, A. M. Johnson, M. Shahmanesh, A. Ozcan, J. J. Collins, M. Fernandez Suarez, B. Rodriguez, R. W. Peeling, R. A. Mckendry, *Nat. Rev. Bioeng.* **2023**, *1*, 13.
[211] Z. S. Ballard, H. A. Joung, A. Goncharov, J. Liang, K. Nugroho, D. di Carlo, O. B. Garner, A. Ozcan, *NPJ Digit. Med.* **2020**, *3*, 66.
[212] O. Mudanyali, S. Dimitrov, U. Sikora, S. Padmanabhan, I. Navruz, A. Ozcan, *Lab Chip* **2012**, *12*, 2678.
[213] Urusov, Zherdev, Dzantiev, *Biosensors* **2019**, *9*, 89.
[214] S. R. Johnson, S. Godbert, P. Perry, P. Parsons, L. Roberts, P. Buchanan, J. Larsen, T. A. Alonzo, M. Zinaman, *Fertil. Steril* **2013**, *100*, 1635.
[215] X. Chen, L. Ding, X. Huang, Y. Xiong, *Theranostics* **2022**, *12*, 574.
[216] R. Banerjee, A. Jaiswal, *Analyst* **2018**, *143*, 1970.
[217] C. Swanson, A. D'andrea, *Clin. Chem.* **2013**, *59*, 641.
[218] J. Park, *Sensors* **2022**, *22*, 7398.
[219] X. Xie, M. C. Nielsen, A. E. Muruato, C. R. Fontes-Garfias, P. Ren, *Diagn. Microbiol. Infect. Dis.* **2021**, *99*, 115248.
[220] J. T. Whicher, C. P. Price, K. Spencer, A. M. Ward, *Crit. Rev. Clin. Lab. Sci.* **1982**, *18*, 213.
[221] K. Kuningas, T. Ukonaho, H. Päkkilä, T. Rantanen, J. Rosenberg, T. Lövgren, T. Soukka, *Anal. Chem.* **2006**, *78*, 4690.
[222] A. M. Quinn, A. Allali-Hassani, M. Vedadi, A. Simeonov, *Mol. BioSyst.* **2010**, *6*, 782.
[223] T. Soukka, J. Paukkunen, H. Härmä, S. Lönnberg, H. Lindroos, T. Lövgren, *Clin. Chem.* **2001**, *47*, 1269.
[224] X. Wang, F. Li, Y. Guo, *Front. Chem.* **2020**, *8*, 586702.
[225] M. Hall, I. Kazakova, Y.-M. Yao, *Anal. Biochem.* **1999**, *272*, 165.
[226] S. Lahtinen, S. Krause, R. Arppe, T. Soukka, T. Vosch, *Chem. - Eur. J.* **2018**, *24*, 9229.
[227] E. F. Ullman, H. Kirakossian, A. C. Switchenko, J. Ishkanian, M. Ericson, C. A. Wartchow, M. Pirio, J. Pease, B. R. Irvin, S. Singh, R. Singh, R. Patel, A. Dafforn, D. Davalian, C. Skold, N. Kurn, D. B. Wagner, *Clin. Chem.* **1996**, *42*, 1518.
[228] J. M. Correira, P. R. Handali, L. J. Webb, *J. Chem. Phys.* **2022**, *157*, 090902.
[229] K. E. Sapsford, K. M. Tyner, B. J. Dair, J. R. Deschamps, I. L. Medintz, *Anal. Chem.* **2011**, *83*, 4453.
[230] B. Saha, T. H. Evers, M. W. J. Prins, *Anal. Chem.* **2014**, *86*, 8158.
[231] V. Gubala, L. F. Harris, A. J. Ricco, M. X. Tan, D. E. Williams, *Anal. Chem.* **2012**, *84*, 487.

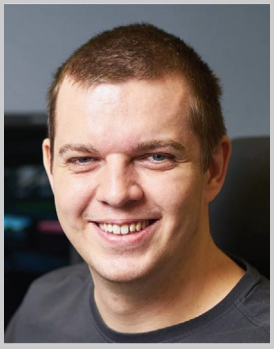

**Zdeněk Farka** works as an associate professor at the Department of Biochemistry, Faculty of Science, Masaryk University, where he leads a research group Immunoassays and Nanosensors. He received his Ph.D. in 2017 at Masaryk University and completed research internships at the University of Regensburg and the University of Rouen. His group develops highly sensitive tools for the detection and visualization of clinically and environmentally important analytes. The group employs various kinds of transducers and labels, with a great focus devoted to nanomaterials, which not only enhance sensitivity but also enable novel detection formats.

**Julian C. Brandmeier** is a Ph.D. student at the Institute of Analytical Chemistry, Chemo- and Biosensors, University of Regensburg, where he received his M.Sc. in 2021. Currently he is on an extended research stay at the Department of Biochemistry, Faculty of Science, Masaryk University Brno. In his Ph.D. project he develops highly sensitive analogue and digital immunoassays using photon-upconversion nanoparticles as detection labels. Furthermore, he specializes in the surface modification of such nanoparticles utilizing a wide variety of reactive groups and biomolecules to increase assay performance and enable new detection methods.

**Matthias J. Mickert** received his doctorate in 2021 from the University of Regensburg, where he conducted research on photon-upconversion nanoparticles as background-free luminescent labels for immunoanalytical applications at the Institute of Analytical Chemistry, Chemo- and Biosensors. He then joined the biotech company Lumito AB in Sweden as a senior chemical engineer, where he develops a reagent kit based on upconverting nanoparticles for the detection of biomarkers in tissue sections.

**Matěj Pastucha** is working on the development of multiplex immunochemical assays in company TestLine Clinical Diagnostics, Czech Republic. He received his M.Sc. in analytical biochemistry in 2015 and is currently pursuing a Ph.D. in biochemistry under the supervision of Petr Skládal at Masaryk University in Brno. His area of expertise is protein conjugation with nanoparticles and other labels or surfaces and their application in immunochemical assays and sensors that employ an optical or electrochemical readout.

**Karel Lacina** received his Ph.D. degree in 2011 at Masaryk University and has been a research fellow there since. He completed research internships at the University of Bath and the State University of New York. His whole career has been devoted to electrochemical biosensors and to electrochemistry in general. Currently at CEITEC Masaryk University, Karel Lacina develops immunoassays with electrochemical detection to transfer the outputs to practice, he collaborates with several industrial partners in the region of Central Europe.

**Petr Skládal** is Professor of Biochemistry and Director of the Department of Biochemistry, Faculty of Science, Masaryk University. He received his Ph.D. in the field of amperometric biosensors in 1992, completed research stays (1991, 1993) at the University of Florence and was visiting professor at the State University of Sao Paulo, Brazil (1996). He founded the Nanobiotechnology Core Laboratory at the Central European Institute of Technology in Brno (2005). His research is focused on enzyme and immunochemical biosensors using electrochemical and piezoelectric transducers, affinity kinetics with surface plasmon resonance systems, and applications of atomic force microscopy in the life sciences.

**Hans H. Gorris** has been an associated professor at the Department of Biochemistry, Faculty of Science, Masaryk University in Brno since 2021. He received his Ph.D. from the University of Lübeck, was a postdoctoral fellow at Tufts University (USA) and a research group leader and Heisenberg Fellow at the University of Regensburg. His main research interests are digital immunoassays based on photon-upconversion nanoparticles (UCNPs) and new methods for investigating enzymes at the single-molecule level.